Applications of Mathematics

Ondřej Čertík; Francesca Gardini; Gianmarco Manzini; Giuseppe Vacca

The virtual element method for eigenvalue problems with potential terms on polytopic meshes

Applications of Mathematics, Vol. 63 (2018), No. 3, 333–365

Persistent URL: http://dml.cz/dmlcz/147314

63 (2018) APPLICATIONS OF MATHEMATICS No. 3, 333–365

THE VIRTUAL ELEMENT METHOD FOR EIGENVALUE PROBLEMS WITH POTENTIAL TERMS ON POLYTOPIC MESHES

Ondřej Čertík, Los Alamos, Francesca Gardini, Pavia,
Gianmarco Manzini, Los Alamos, Giuseppe Vacca, Milano

Received March 31, 2018. Published online July 2, 2018.

Abstract. We extend the conforming virtual element method (VEM) to the numerical resolution of eigenvalue problems with potential terms on a polytopic mesh. An important application is that of the Schrödinger equation with a pseudopotential term. This model is a fundamental element in the numerical resolution of more complex problems from the Density Functional Theory. The VEM is based on the construction of the discrete bilinear forms of the variational formulation through certain polynomial projection operators that are directly computable from the degrees of freedom. The method shows a great flexibility with respect to the meshes and provides a correct spectral approximation with optimal convergence rates. This point is discussed from both the theoretical and the numerical viewpoint. The performance of the method is numerically investigated by solving the quantum harmonic oscillator problem with the harmonic potential and a singular eigenvalue problem with zero potential for the first eigenvalues.

Keywords: conforming virtual element; eigenvalue problem; Hamiltonian equation; polygonal mesh

MSC 2010: 65L15, 65L60, 65L70

The work of the first and third author was supported by the Laboratory Directed Research and Development Program (LDRD), U.S. Department of Energy Office of Science, Office of Fusion Energy Sciences, and the DOE Office of Science Advanced Scientific Computing Research (ASCR) Program in Applied Mathematics Research, under the auspices of the National Nuclear Security Administration of the U.S. Department of Energy by Los Alamos National Laboratory, operated by Los Alamos National Security LLC under contract DE-AC52-06NA25396. The fourth author was partially supported by the European Research Council through the H2020 Consolidator Grant (grant no. 681162) CAVE—Challenges and Advancements in Virtual Elements. This support is gratefully acknowledged.

DOI: 10.21136/AM.2018.0093-18

1. Introduction

The numerical treatment of the Schrödinger equation with local pseudopotentials is one of the most expensive steps in solving electronic-structures in large-scale Density Functional calculations, see e.g. [10], [42], [59]. These calculations make it possible to determine properties of materials from quantum-mechanical first principles (ab initio), hence without the need of adaptable parameters. A widely used approach for solving the Schrödinger equation in large-scale quantum-mechanical physical systems is provided by *the plane wave (PW) pseudopotential method* [54] and its many variants. PW methods are spectral methods based on an expansion on Fourier basis functions (the plane waves). Such methods are generally accurate, but their computer implementation may be inefficient as it normally relies on the *fast Fourier transform (FFT)*, whose nonlocal communication pattern compromises the method's scalability on parallel architectures. Moreover, the strictly uniform resolution of a plane waves expansion makes resolution adaptation infeasible, thus requiring to consider a big number of PWs to capture the highly oscillatory behavior in the atomic region. Such a high resolution is unnecessary in transition regions between atoms where the solution to the Schrödinger equation is normally much smoother. This fact may eventually lead to computationally inefficient discretizations [52].

An alternative to the PW approach has been offered in recent years by real-space methods such as finite differences, finite volumes, and finite elements. Such methods are based on the direct approximation of the solution of the Schrödinger equation on a computational grid. In particular, the finite element method (FEM) is a variational method based on the expansion of the solution in shape basis functions, usually piecewise polynomials that are strictly locally defined in each mesh element. As noted in [50], [51], the strictly local nature of the shape functions has several important consequences. First, the FEM produces sparse matrices that can efficiently be treated by standard iterative methods (preconditioned Krylov schemes) [30]; the computational mesh can be refined near the atom locations, where the eigenfunctions are expected to vary the most in order to increase the efficiency of the representation; highly scalable implementations are possible on parallel machines. Moreover, the accuracy of the method can easily be improved by increasing the polynomial degree of the shape functions and systematically enhanced by adding other nonpolynomial functions, which incorporates in the local approximation some physical insight from the eigenfunction behaviour [53], [55].

A very recent and important development in the field of the FEM consists in the virtual element method (VEM), which was introduced in [11] as a variational reformulation of the Mimetic Finite Difference (MFD) method [18], [19], [44]. The VEM is a very successful approach for the construction of numerical approximation

of any order of accuracy and regularity on general polygonal/polyhedral meshes. Despite its relative recentness (the first paper was published in 2013), the VEM has been developed successfully for a large range of mathematical and engineering problems [6], [4], [7], [12], [23], [16], [20], [21], [26], [33], [35], [56], [57], [58], extended to curved edges [25], and three dimensional problems [3], [17], [36], using also mixed spaces [29] and nonconforming spaces [5], [8], [32], [34], [45]. High-order and higher-order continuity schemes have been presented in [16] and [4], [22], [28], respectively.

The VEM is indeed a finite element method, so all good properties of the FEM when applied to the Schrödinger equation still hold. In addition, we can exploit the great flexibility of the method, which comes from the fact that the shape functions used in the variational formulation are not known in a closed form, but are defined as the solution of suitable differential problems. This fact is also the motivation of the name "virtual".

The construction of the method and its practical implementations rely on the special choice of the degrees of freedom rather than the explicit knowledge of the local shape functions. The degrees of freedom allow the calculation of certain projection operators from local virtual element spaces into polynomial subspaces. Using such operators, we can properly construct the discrete bilinear forms that approximate the continuous ones of the variational formulation in the virtual element framework.

The present work is the first instance of a long term project that aims at extending the virtual element approach to the real-space numerical approximation of the equations of the Density Functional Theory. We start here by considering the Schrödinger equation with local pseudopotentials and Dirichlet/Neumann boundary conditions. Despite its simplicity, this model allows us to compute the spectrum of the classical quantum harmonic oscillator. We emphasize that the zero potential case, which corresponds to the standard eigenvalue problem for the Laplace operator, also provides the classical "atom in a box" model. Previous works investigating the VEM for eigenvalue problems regard the approximation of the Steklov eigenvalue problem [46], [47], the Laplace eigenvalue problem [40], [39] with conforming and nonconforming virtual elements, respectively, the acoustic vibration problem [24], the vibration problem of Kirchhoff plates [48], the transmission eigenvalue problem [49], whereas [31] deals with the Mimetic Finite Difference approximation of the eigenvalue problem in mixed form.

The outline of the paper is as follows. In Section 2 we recall the eigenvalue problem under investigation, introducing the classical variational formulation and the necessary notation. Section 3 details the proposed discretization procedure. The approximation spaces and all the bilinear forms that define the discrete problem are introduced and described. Section 4 deals with the theoretical analysis, which leads to the optimal error estimates of Theorems 4.5, 4.6, and 4.7. In Section 5

we present several numerical tests which highlight the actual performance of our approach. Finally, in Section 6 we offer our final remarks and conclusions.

2. The continuous eigenvalue problem

2.1. Technicalities and definitions. We use the standard definition and notation of Sobolev spaces, norms and seminorms as given in [1]. Hence, the Sobolev space $H^s(\omega)$ consists of functions defined on an open bounded connected subset ω of $\mathbb{R}^d$, $d = 1, 2, 3$, that are square integrable and whose weak derivatives up to order s are also square integrable. As usual, if $s = 0$, we prefer the notation $L^2(\omega)$. Norm and seminorm in $H^s(\omega)$ are denoted by $\|\cdot\|_{s,\omega}$ and $|\cdot|_{s,\omega}$, respectively, and $(\cdot,\cdot)_\omega$ denotes the L^2-inner product. The subscript ω may be omitted when ω is the whole computational domain Ω.

If $l \geqslant 0$ is an integer number, $\mathbb{P}_l(\omega)$ is the space of polynomials of degree up to l defined on ω, with the convention that $\mathbb{P}_{-1}(\omega) = \{0\}$. The L^2-orthogonal projection onto the polynomial space $\mathbb{P}_l(\omega)$ is denoted by $\Pi_l^{0,\omega}\colon L^2(\omega) \to \mathbb{P}_l(\omega)$. The space $\mathbb{P}_l(\omega)$ is the span of the finite set of *scaled monomials of degree up to* l, that are given by

$$\mathcal{M}_l(\omega) = \{((\mathbf{x} - \mathbf{x}_\omega)/h_\omega)^\alpha \text{ with } |\alpha| \leqslant l\}, \tag{2.1}$$

where

- $\mathbf{x}_\omega$ denotes the center of gravity of ω and h_ω its characteristic length, as, for instance, the edge length, the face diameter, or the cell diameter for $d = 1, 2, 3$;
- $\alpha = (\alpha_1, \ldots, \alpha_d)$ is the d-dimensional multi-index of nonnegative integers α_i with degree $|\alpha| = \alpha_1 + \ldots + \alpha_d \leqslant l$ and such that $\mathbf{x}^\alpha = x_1^{\alpha_1} \ldots x_d^{\alpha_d}$ for any $\mathbf{x} \in \mathbb{R}^d$.

We will also use the set of *scaled monomials of degree exactly equal to* l, denoted by $\mathcal{M}_l^*(\omega)$ and obtained by setting $|\alpha| = l$ in the definition above.

Finally, we use the letter C in the estimates throughout the paper to denote a strictly positive constant that is independent of the mesh size h, but may depend on the problem constants, like the coercivity and continuity constants, or other discretization constants like the mesh regularity constant, the stability constants, etc. The constant C generally has a different value at each occurrence.

2.2. The continuous model. Let $\Omega \subseteq \mathbb{R}^d$ for $d = 2, 3$ be the computational domain and let Γ be the boundary of Ω. We are interested in the numerical approximation of the eigenvalues $\lambda \in \mathbb{R}$ and the eigenfunctions $u\colon \Omega \to \mathbb{R}$, $u \neq 0$, solving the problem in strong form

$$-\tfrac{1}{2}\Delta u(\mathbf{x}) + V(\mathbf{x})u(\mathbf{x}) = \lambda u(\mathbf{x}), \quad \mathbf{x} \in \Omega, \tag{2.2}$$

where $V(\mathbf{x})$ is a smooth real-valued scalar potential function. In the context of atomic and molecular quantum theory, λ and u are the energy level and the corresponding wavefunction of the Hamilton operator $\mathcal{H} := -\frac{1}{2}\Delta + V(\mathbf{x})$, and potential $V(\mathbf{x})$ collects all local and nonlocal terms from the Density Functional Theory [10], [42], [59]. For a proper mathematical formulation, problem (2.2) is supplemented with suitable boundary conditions that, depending on the problem, can be of Dirichlet, Neumann, or periodic type (if Ω is a parallelepiped). In the following we consider for sake of simplicity homogeneous Dirichlet boundary conditions. The other cases easily follow the same construction. Furthermore we assume that $V(\mathbf{x})$ is uniformly bounded from below and from above, i.e., there exist two strictly positive constants V_* and V^* such that $V_* \leqslant V(\mathbf{x}) \leqslant V^*$ for almost every $\mathbf{x} \in \Omega$.

The variational formulation of (2.2) reads: *Find* $\lambda \in \mathbb{R}$ *and* $u \in H_0^1(\Omega)$, $\|u\|_{L^2(\Omega)} = 1$, *such that*

$$a(u, v) = \lambda b(u, v) \quad \forall\, v \in H_0^1(\Omega), \tag{2.3}$$

where the bilinear form $a\colon\ H^1(\Omega) \times H^1(\Omega) \to \mathbb{R}$ is given by

$$a(u, v) = \int_\Omega \big(\tfrac{1}{2}\nabla v(\mathbf{x}) \cdot \nabla u(\mathbf{x}) + V(\mathbf{x})u(\mathbf{x})v(\mathbf{x})\big)\,\mathrm{d}\mathbf{x} \quad \forall\, u,\, v \in H^1(\Omega), \tag{2.4}$$

and the bilinear form $b\colon\ L^2(\Omega) \times L^2(\Omega) \to \mathbb{R}$ is the L^2-inner product on Ω, i.e.,

$$b(u, v) = \int_\Omega u(\mathbf{x})v(\mathbf{x})\,\mathrm{d}\mathbf{x} \quad \forall u,\, v \in L^2(\Omega). \tag{2.5}$$

R e m a r k 2.1. From the standard eigenvalue theory, see [9], [27], we know that

(i) problem (2.3) admits a discrete infinite set of eigenvalues forming a positive increasing divergent sequence;

(ii) the corresponding eigenfunctions are an orthonormal basis of $H_0^1(\Omega)$ with respect to the L^2-inner product and the scalar product associated with the bilinear form $a(\cdot, \cdot)$;

(iii) the eigenvalues may have multiplicity bigger than one, but in such a case the corresponding eigenspace must have finite dimension.

We also consider the source problem with homogeneous Dirichlet boundary conditions: *Find* $u^s \in H_0^1(\Omega)$ *such that*

$$a(u^s, v) = b(g, v) \quad \forall\, v \in H_0^1(\Omega), \tag{2.6}$$

where we assume that $g \in L^2(\Omega)$. Well-posedness of problem (2.6), i.e., the existence and uniqueness of its solution, is proved by using the Lax-Milgram Lemma [38] since,

due to the boundedness assumption on the potential field V, the bilinear form a in (2.4) is coercive and the bilinear form b in (2.5) is continuous. Moreover, due to a regularity result [2], [41], there exists $r > 0$, depending only on Ω, such that $u^s \in H^{1+r}(\Omega)$. Eventually, the following stability estimate holds:

$$|u^s|_{1+r} \leqslant C\|g\|_0. \tag{2.7}$$

3. The virtual element method

We are interested in developing the virtual element approximation of the eigenvalue problem in variational form (2.3). To this end, we first discuss which meshes can be used for the numerical formulation and introduce a proper set of regularity assumptions. Then, we define the local and global virtual element spaces, the degrees of freedom and the bilinear forms a_h and b_h that approximate a and b. Finally, we review the estimate of the convergence rate for the related VEM approximation of the source problem.

3.1. Mesh definition and regularity assumptions. Let Ω_h denote a decomposition of the computational domain Ω into a finite set of polytopic elements P. As usual, the subindex h that labels the mesh Ω_h is the maximum of the diameters $h_P = \sup_{\mathbf{x},\mathbf{y}\in P} |\mathbf{x}-\mathbf{y}|$ of the elements of the mesh. We assume that the elements are nonoverlapping and for each element P we denote its $(d-1)$-dimensional nonintersecting boundary by ∂P, its center of gravity by $\mathbf{x}_P$, its d-dimensional measure by $|P|$. The boundary of P is formed by straight edges when $d = 2$ and flat faces when $d = 3$. On 3D polyhedral meshes, we denote the midpoint and length of each mesh edge e by $\mathbf{x}_e$ and h_e, respectively, and the center of gravity, diameter and area of each face f are denoted by $\mathbf{x}_f$, h_f, and $|f|$, respectively. In the 2D case, we do not make any special distinction between the terms "*edge*" and "*face*", which we consider as synonyms. To unify the notation we may use the symbol σ instead of e or f and, for example, refer to the geometric objects forming the elemental boundary ∂P by the term *side* instead of *edge*/*face*. According to such notation, we denote the center of gravity, diameter, and measure of side σ by $\mathbf{x}_\sigma$, h_σ, and $|\sigma|$, respectively.

Consider the set $\mathcal{T} = \{\Omega_h\}_h$ formed by the decompositions of Ω for $h \to 0$. The convergence analysis of the conforming VEM, we want to consider in this work, requires some regularity assumptions that must be satisfied by all members of the mesh family $\mathcal{T}$. For completeness we state these assumptions for both $d = 2$ and $d = 3$ cases, although those for $d = 2$ can be derived from those for $d = 3$ by reducing the spatial dimension.

(A0) Mesh regularity assumptions.

- ▷ $d = 3$. There exists a positive constant ϱ independent of h (and, hence, of Ω_h) such that for every polyhedral element $P \in \Omega_h$ it holds that
  - (i) P is star-shaped with respect to a ball with radius $\geqslant \varrho h_P$,
  - (ii) every face $f \in P$ is star-shaped with respect to a disk with radius $\geqslant \varrho h_f$,
  - (iii) for every edge $e \in \partial f$ of every face $f \in \partial P$ it holds that $h_e \geqslant \varrho h_f \geqslant \varrho^2 h_P$,
- ▷ $d = 2$. There exists a positive constant ϱ independent of h (and, hence, of Ω_h) such that for every polygonal element $P \in \Omega_h$ it holds that
  - (i) P is star-shaped with respect to a disk with radius $\geqslant \varrho h_P$,
  - (ii) for every edge $e \in \partial P$ it holds that $h_e \geqslant \varrho h_P$.

The scaling assumption implies that the number of edges and faces in each elemental boundary is uniformly bounded over the whole mesh family $\{\Omega_h\}$. The star-shapedness property implies that the elements and faces are *simply connected* subsets of $\mathbb{R}^d$ and $\mathbb{R}^{d-1}$, respectively.

3.2. The conforming virtual element space. We construct the local conforming virtual element space by resorting to the so-called *enhancement strategy* introduced in [3]. The construction of the conforming virtual element space in the multidimensional case for $d \geqslant 3$ is recursive. We discuss here only the more general case for $d = 3$, while the case for $d = 2$ follows from a simple dimensional reduction.

To this end, on every polygonal face f of the boundary ∂P and for any integer number $k \geqslant 1$ we first define the finite element space

$$\widetilde{V}_k^h(f) = \{v_h \in H^1(f) \cap C^0(\overline{f})\colon\ v_{h|\partial f} \in C^0(\partial f),\ v_{h|e} \in \mathbb{P}_k(e) \quad \forall\, e \subset \partial f,\ \Delta v_h \in \mathbb{P}_k(f)\,\}. \tag{3.1}$$

It is worth noting that the space of polynomials of degree up to k defined on f is a subspace of $\widetilde{V}_k^h(f)$. Then, we introduce the set of continuous linear functionals from $\widetilde{V}_k^h(f)$ to $\mathbb{R}$ that for every virtual function v_h of $\widetilde{V}_k^h(f)$ provide:

(D1) the values of v_h at the vertices of f,

(D2) the moments of v_h of order up to $k-2$ on each one-dimensional edge $e \in \partial f$:

$$\frac{1}{|e|}\int_e v_h\, m \,\mathrm{d}\sigma \quad \forall\, m \in \mathcal{M}_{k-2}(e) \quad \forall\, e \in \partial f, \tag{3.2}$$

(D3) the moments of v_h of order up to $k-2$ on each two-dimensional face f:

$$\frac{1}{|f|}\int_f v_h\, m \,\mathrm{d}\sigma \quad \forall\, m \in \mathcal{M}_{k-2}(f). \tag{3.3}$$

Finally, we introduce the elliptic projection operator $\Pi_k^{\nabla,f}\colon\ \widetilde{V}_k^h(f) \to \mathbb{P}_k(f)$ that for any $v_h \in \widetilde{V}_k^h(f)$ is defined by:

$$\int_f \nabla \Pi_k^{\nabla,f} v_h \cdot \nabla q \,\mathrm{d}\mathbf{x} = \int_f \nabla v_h \cdot \nabla q \,\mathrm{d}\mathbf{x} \quad \forall\, q \in \mathbb{P}_k(f) \tag{3.4}$$

together with the additional conditions

$$\int_{\partial P} (\Pi_k^{\nabla,f} v_h - v_h) \,\mathrm{d}\sigma = 0 \quad \text{if } k = 1, \tag{3.5}$$

$$\int_P (\Pi_k^{\nabla,f} v_h - v_h) \,\mathrm{d}\mathbf{x} = 0 \quad \text{if } k \geqslant 2. \tag{3.6}$$

As proved in [11], [34], the polynomial projection $\Pi_k^{\nabla,f} v_h$ is computable from the values of the linear functionals (D1)–(D3). Furthermore, $\Pi_k^{\nabla,f}$ is a polynomial-preserving operator, i.e. $\Pi_k^{\nabla,f} q = q$ for every $q \in \mathbb{P}_k(f)$.

The *local conforming virtual element space of order* k on the polygonal face f is the subspace of $\widetilde{V}_k^h(f)$ defined as

$$V_k^h(f) = \{v_h \in \widetilde{V}_k^h(f)\colon\ (v_h - \Pi_k^{\nabla,f} v_h, m)_f = 0 \quad \forall\, m \in \mathcal{M}_{k-1}^*(f) \cup \mathcal{M}_k^*(f)\}. \tag{3.7}$$

Space $V_k^h(f)$ has two important properties that we outline below:

(i) it still contains the space of polynomials of degree at most k,

(ii) the values provided by the set of continuous linear functionals (D1)–(D3) uniquely determine every function v_h of $V_k^h(f)$ and can be taken as the *degrees of freedom* of v_h.

Property (i) above is a direct consequence of the space definition, while property (ii) follows from the unisolvability of the degrees of freedom (D1)–(D3) that was proved in [3].

R e m a r k 3.1. Additionally, from the space definition, we have that the L^2-orthogonal projection $\Pi_k^{0,f} v_h$ is computable exactly using only the degrees of freedom of v_h, and $\Pi_k^{0,f} v_h = \Pi_k^{\nabla,f} v_h$ for $k = 1, 2$.

To define the conforming virtual element space on the polyhedral cell P, we first need to introduce the "*extended*" virtual element space:

$$\widetilde{V}_k^h(P) = \{v_h \in H^1(P) \cap C^0(\overline{P})\colon\ v_{h|\partial P} \in C^0(\partial P),\ v_{h|f} \in V_k^h(f) \quad \forall\, f \subset \partial P,\ \Delta v_h \in \mathbb{P}_k(P)\}. \tag{3.8}$$

The space $\widetilde{V}_k^h(P)$ clearly contains the polynomials of degree k. Now we introduce the set of continuous linear functionals from $\widetilde{V}_k^h(P)$ to $\mathbb{R}$ that are the obvious three-dimensional counterparts of the linear operators of the bi-dimensional case. For every virtual function v_h of $\widetilde{V}_k^h(P)$ we provide [3], [17]:

(D1) the values of v_h at the vertices of P,

(D2) the moments of v_h of order up to $k-2$ on each one-dimensional edge $e \in \partial P$:

$$\frac{1}{|e|}\int_e v_h m \,\mathrm{d}\sigma \quad \forall\, m \in \mathcal{M}_{k-2}(e) \quad \forall\, e \in \partial P, \tag{3.9}$$

(D3) the moments of v_h of order up to $k-2$ on each two-dimensional face $f \in \partial P$:

$$\frac{1}{|f|}\int_f v_h\, m \,\mathrm{d}\sigma \quad \forall\, m \in \mathcal{M}_{k-2}(f) \quad \forall\, f \in \partial P, \tag{3.10}$$

(D4) the moments of v_h of order up to $k-2$ on P:

$$\frac{1}{|P|}\int_P v_h m \,\mathrm{d}\mathbf{x} \quad \forall\, m \in \mathcal{M}_{k-2}(P). \tag{3.11}$$

Then we introduce the H^1-seminorm projection operator $\Pi_k^{\nabla,P}\colon\ \widetilde{V}_k^h(P) \to \mathbb{P}_k(P)$ that for any $v_h \in \widetilde{V}_k^h(P)$ is defined by

$$\int_P \nabla\Pi_k^{\nabla,P} v_h \cdot \nabla q \,\mathrm{d}\mathbf{x} = \int_P \nabla v_h \cdot \nabla q \,\mathrm{d}\mathbf{x} \quad \forall\, q \in \mathbb{P}_k(P) \tag{3.12}$$

coupled with the conditions

$$\int_{\partial P} (\Pi_k^{\nabla,P} v_h - v_h) \,\mathrm{d}\sigma = 0 \quad \text{if } k = 1, \tag{3.13}$$

$$\int_P (\Pi_k^{\nabla,P} v_h - v_h) \,\mathrm{d}\mathbf{x} = 0 \quad \text{if } k \geqslant 2. \tag{3.14}$$

The polynomial projection $\Pi_k^{\nabla,P} v_h$ can be computed in terms of the values of the linear functionals (D1)–(D4). Finally, $\Pi_k^{\nabla,P}$ is polynomial-preserving, i.e. $\Pi_k^{\nabla,P} q = q$ for every $q \in \mathbb{P}_k(P)$.

We are now ready to introduce the *local conforming virtual element space of order* k on the polytopic element P, which is the subspace of $\widetilde{V}_k^h(P)$ defined as follows:

$$V_k^h(P) = \{v_h \in \widetilde{V}_k^h(P)\colon\ (v_h - \Pi_k^{\nabla,P} v_h, m)_P = 0\ \forall\, m \in \mathcal{M}_{k-1}^*(P) \cup \mathcal{M}_k^*(P)\}. \tag{3.15}$$

We recall that, by construction, the local space $V_k^h(P)$ enjoys the following fundamental properties (see [3], [17]):

(i) it still contains the space of polynomials of degree at most k,

(ii) the values provided by the set of continuous linear functionals (D1)–(D4) uniquely determine every function v_h of $V_k^h(P)$ and can be taken as the *degrees of freedom* of v_h,

(iii) we can define an interpolation operator in $V_k^h(P)$ with optimal approximation properties so that for every $v \in H^{r+1}(P)$ with $1 \leqslant r \leqslant k$ the interpolant v^{I} satisfies the inequality

$$\|v - v^{\mathrm{I}}\|_{L^2(P)} + h_P |v - v^{\mathrm{I}}|_{H^1(P)} \leqslant C h_P^{r+1} |v|_{H^{r+1}(P)} \tag{3.16}$$

for some positive constant C independent of h.

As for the 2D case, the L^2-orthogonal projection $\Pi_k^{0,P} v_h$ is computable in terms of the degrees of freedom of v_h, and $\Pi_k^{0,P} v_h = \Pi_k^{\nabla,P} v_h$ for $k = 1, 2$.

Finally, the *global conforming virtual element space* V_k^h *of order* $k \geqslant 1$ *subordinate to the mesh* Ω_h is obtained by gluing together the elemental spaces $V_k^h(P)$ to form a subspace of the conforming space $H^1(\Omega)$. The formal definition reads

$$V_k^h := \{v_h \in H_0^1(\Omega) \colon\ v_{h|P} \in V_k^h(P) \quad \forall\, P \in \Omega_h\}. \tag{3.17}$$

A set of degrees of freedom for V_k^h is given by collecting the values from the linear functionals (D1)–(D4) for all the mesh elements. The unisolvability of such degrees of freedom is an immediate consequence of their unisolvability on each local space $V_k^h(P)$.

3.3. The VEM for the eigenvalue problem. The next step in the construction of our method is to define a discrete version of the bilinear forms a and b given in (2.4) and (2.5). First of all we split the bilinear form a into the sum of local terms:

$$a(u, v) = \sum_{P \in \Omega_h} a^P(u, v), \quad \text{where } a^P(u, v) = \int_P \big(\tfrac{1}{2} \nabla u \cdot \nabla v + V u v\big)\, \mathrm{d}\mathbf{x}, \tag{3.18}$$

and we note that for an arbitrary pair $(u, v) \in V_k^h \times V_k^h$ the quantity $a(u, v)$ is not computable. Then, following a standard procedure in the VEM framework, we consider a computable discrete local bilinear form $a_h(\cdot, \cdot)$ given by the sum of elemental contributions

$$a_h(u_h, v_h) = \sum_{P \in \Omega_h} a_h^P(u_h, v_h), \tag{3.19}$$

where we define

$$\begin{aligned} a_h^P(u_h, v_h) = {} & \frac{1}{2} \int_P \Pi_{k-1}^{0,P} \nabla u_h \cdot \Pi_{k-1}^{0,P} \nabla v_h \, \mathrm{d}\mathbf{x} \\ & + \int_P V \Pi_k^{0,P} u_h \, \Pi_k^{0,P} v_h \, \mathrm{d}\mathbf{x} + S^P((I - \Pi_k^{\nabla,P}) u_h, \big(I - \Pi_k^{\nabla,P}\big) v_h), \end{aligned} \tag{3.20}$$

$S^P(\cdot,\cdot)$ being the stabilization term that will be discussed in the following. The bilinear form a_h^P depends on the orthogonal projections $\Pi_{k-1}^{0,P}\nabla u_h$ and $\Pi_{k-1}^{0,P}\nabla v_h$, which are computable from the degrees of freedom of u_h and v_h, respectively [3]. In fact, starting from the definition of the orthogonal projection, integration by parts yields

$$\begin{aligned}\int_P \Pi_{k-1}^{0,P}\nabla u_h\cdot\mathbf{q}\,\mathrm{d}V &= \int_P \nabla u_h\cdot\mathbf{q}\,\mathrm{d}V \quad \forall\,\mathbf{q}\in[\mathbb{P}_{k-1}(P)]^d\\ &= -\int_P u_h\nabla\cdot\mathbf{q}\,\mathrm{d}V+\sum_{f\in\partial P}\int_f u_h\mathbf{n}_{P,f}\cdot\mathbf{q}\,\mathrm{d}\sigma,\end{aligned}\tag{3.21}$$

where $\mathbf{n}_{P,f}$ denotes the unit outward normal to f. The first integral on the last right-hand side is computable from the degrees of freedom (D4) as it is the moment of u_h against a polynomial of degree $k-2$ over P. The face integrals above are also computable, since

$$\int_f u_h\mathbf{n}_{P,f}\cdot\mathbf{q}\,\mathrm{d}\sigma=\int_f \Pi_{k-1}^{0,f}u_h\mathbf{n}_{P,f}\cdot\mathbf{q}\,\mathrm{d}\sigma$$

and the L^2-orthogonal projection $\Pi_{k-1}^{0,f}u_h$, as we have seen, is computable exactly using only the degrees of freedom of u_h, cf. Remark 3.1.

The discrete form $a_h^P(\cdot,\cdot)$ must satisfy two fundamental properties:

▷ *k-consistency*: for all $v_h\in V_k^h$ and for all $q\in\mathbb{P}_k(P)$ it holds

$$a_h^P(v_h,q)=a^P(v_h,q);\tag{3.22}$$

▷ *stability*: there exist two positive constants α_*, α^*, independent of h and of P, such that

$$\alpha_* a^P(v_h,v_h)\leqslant a_h^P(v_h,v_h)\leqslant\alpha^* a^P(v_h,v_h)\quad\forall\,v_h\in V_k^h.\tag{3.23}$$

Stability is ensured by adding the bilinear form S^P, which can be any symmetric positive definite bilinear form on the element P for which there exist two positive constants c_* and c^* such that

$$c_* a^P(v_h,v_h)\leqslant S^P(v_h,v_h)\leqslant c^* a^P(v_h,v_h)\quad\forall\,v_h\in V_k^h(P)\text{ with }\Pi_k^{\nabla,P}v_h=0.\tag{3.24}$$

Note that $S^P(\cdot,\cdot)$ must scale like $a^P(\cdot,\cdot)$, namely $S^P(\cdot,\cdot)\simeq h_P^{d-2}$ (see also Section 5).

Following [39], [40], we consider two different discretizations of the eigenvalue problem (2.3) that are obtained by considering two possible choices for the discretization of the bilinear form b (cf. (2.5)). We split b into the local contributions

$$b(u,v) = \sum_{P\in\Omega_h} b^P(u,v), \text{ where } b^P(u,v) = \int_P u(\mathbf{x})v(\mathbf{x})\,\mathrm{d}\mathbf{x}. \tag{3.25}$$

In the first choice we consider an approximated bilinear form b_h, which satisfies the k-consistency property but not the stability property (extending to b_h the definitions above). Therefore, we simply take

$$b_h^P(u_h,v_h) = \int_P \Pi_k^{0,P}u_h\Pi_k^{0,P}v_h\,\mathrm{d}\mathbf{x}. \tag{3.26}$$

The second possible choice consists in considering a discrete bilinear form $\tilde{b}_h(\cdot,\cdot)$ which, as done for the discrete form $a_h(\cdot,\cdot)$, enjoys both the k-consistency property and the stability property. In particular, we define

$$\tilde{b}_h^P(u_h,v_h) = \int_P \Pi_k^{0,P}u_h\,\Pi_k^{0,P}v_h\,\mathrm{d}\mathbf{x} + \widetilde{S}^P((I-\Pi_k^{0,P})u_h,(I-\Pi_k^{0,P})v_h), \tag{3.27}$$

where $\widetilde{S}^P$ is any positive definite bilinear form on the element P such that there exist two uniform positive constants β_* and β^* such that

$$\beta_* b^P(v_h,v_h) \leqslant \widetilde{S}^P(v_h,v_h) \leqslant \beta^*\, b^P(v_h,v_h) \quad \forall\, v_h \in V_h^k(P) \text{ with } \Pi_k^{0,P}v_h = 0.$$

R e m a r k 3.2. In analogy with the condition on the form $S^P(\cdot,\cdot)$, we require that the form $\widetilde{S}^P(\cdot,\cdot)$ scales like $b^P(\cdot,\cdot)$, that is $\widetilde{S}^P(\cdot,\cdot) \simeq h^d$.

The resulting virtual element scheme reads: *Find* $(\lambda_h,u_h)\in\mathbb{R}\times V_k^h$, $\|u_h\|_0 = 1$, *such that*

$$a_h(u_h,v_h) = \lambda_h b_h(u_h,v_h) \quad \forall\, v_h \in V_k^h \tag{3.28}$$

if we adopt the first choice b_h for the approximation of b.

The second virtual element formulation reads: *Find* $(\widetilde{\lambda}_h,\widetilde{u}_h)\in\mathbb{R}\times V_k^h$, $\|\widetilde{u}_h\|_0 = 1$, *such that*

$$a_h(\widetilde{u}_h,v_h) = \widetilde{\lambda}_h\widetilde{b}_h(\widetilde{u}_h,v_h) \quad \forall\, v_h \in V_k^h, \tag{3.29}$$

where we consider the stabilized bilinear form $\widetilde{b}_h$.

Finally, in what follows, we will also need the discrete source problem corresponding to both discrete formulations (3.28) and (3.29), which reads, respectively: *Find* $u_h^s \in V_k^h$ *such that*

$$a_h(u_h^s, v_h) = b_h(g, v_h) \quad \forall\, v_h \in V_k^h \tag{3.30}$$

and *find* $\tilde{u}_h^s \in V_k^h$ *such that*

$$a_h(\tilde{u}_h^s, v_h) = \widetilde{b}_h(g, v_h) \quad \forall\, v_h \in V_k^h. \tag{3.31}$$

The well-posedness of the discrete formulations (3.30) and (3.31) stem from the coercivity of the bilinear form a_h and from the continuity of the forms b_h and $\widetilde{b}_h$.

We finally observe that both bilinear forms are fully computable for any couple of functions $(u_h, v_h) \in V_k^h$, since the enhancement technique implies that $\Pi_k^{0,P} u_h$ and $\Pi_k^{0,P} v_h$ can be computed using only the degrees of freedom of u_h and v_h, respectively.

The following convergence estimate theorem holds for the approximation of the source problem [3].

Theorem 3.3. *Let $u^s \in H^{r+1}(\Omega)$ be the solution to the variational problem* (2.6) *with $g \in L^2(\Omega)$. Let $u_h^s \in V_k^h$ be the solution of the virtual element method* (3.30), *$\tilde{u}_h^s \in V_k^h$ be the solution of the virtual element method* (3.31) *and denote by g_h the piecewise L^2-projection of g onto the space $\mathbb{P}_k(P)$. Under the mesh regularity assumption* (A0), *let $t = \min(k, r)$, and $v_h \in \{u_h^s, \tilde{u}_h^s\}$. Then we have*

▷ *H^1-error estimate:*

$$|u^s - v_h|_{H^1(\Omega)} \leqslant C(h^t |u^s|_{H^{r+1}(\Omega)} + h\|g - g_h\|_{L^2(\Omega)}), \tag{3.32}$$

▷ *L^2-error estimate (for a convex Ω):*

$$\|u^s - v_h\|_{L^2(\Omega)} \leqslant C(h^{t+1} |u^s|_{H^{r+1}(\Omega)} + h\|g - g_h\|_{L^2(\Omega)}). \tag{3.33}$$

R e m a r k 3.4. Note that if u^s is an eigenfunction of the continuous eigenvalue problem (2.3), then it solves the continuous source problem (2.6) with datum λu^s and thus it belongs to $H^{1+r}(\Omega)$ with $|u^s|_{1+r} \leqslant C\|u^s\|_0$ and C depending on λ. Then, recalling that $\|u^s\|_0 = 1$, the a priori error estimates in Theorem 3.3 reduce to

▷ H^1-error estimate:

$$|u^s - v_h|_1 \leqslant C\bigg(h^t |u^s|_{1+r} + h \sum_{P \in \Omega_h} \|(I - \Pi_k^{0,P}) u^s\|_0 \bigg) \leqslant h^t |u^s|_{1+r} \leqslant C h^t \|u^s\|_0 \leqslant C h^t,$$

with C constant depending on the eigenvalue λ,

▷ L^2-error estimate (for a convex Ω):

$$\begin{aligned}\|u^s - v_h\|_0 &\leqslant C\bigg(h^{t+1}|u^s|_{1+r} + h\sum_{P\in\Omega_h}\|(I-\Pi_k^{0,P})u^s\|_0\bigg) \leqslant Ch^{t+1}|u^s|_{1+r}\\ &\leqslant Ch^{t+1}\|u^s\|_0 \leqslant Ch^{t+1}\end{aligned}$$

with C constant depending on the eigenvalue λ.

Indeed,

$$\|(I-\Pi_k^{0,P})u^s\|_0 \leqslant Ch^{\min\{k+1,1+r\}}|u^s|_{1+r} \leqslant Ch^{t+1}\|u^s\|_0.$$

R e m a r k 3.5. We emphasize the two major differences between the virtual element methods (3.28) and (3.29) and those introduced in [40]:

(1) the $V(\mathbf{x})$ term; even if its presence does not pose any real technical difficulty (because we know how to treat it in the VEM), it paves the way to a new set of problems closer to real applications such as the Schrödinger equations,
(2) the VEM with the external projection of the gradients, which is more suitable to treat the Poisson operators with variable coefficients (see [15]).

4. Convergence analysis and error estimates

4.1. Spectral approximation for compact operators. In this section, we briefly recall the results of the spectral approximation theory for compact operators. For more general results, we refer to the original papers [9], [27], [43].

We introduce a natural compact operator associated with problem (2.3) and its discrete counterpart, and we recall their connection with the eigenmode convergence.

Let $T \in \mathcal{L}(L^2(\Omega))$ be the solution operator associated with problem (2.3). The operator $T\colon\ L^2(\Omega) \to L^2(\Omega)$ is bounded, linear, and maps the forcing term g to $u^s =: Tg$:

$$\begin{cases} Tg \in H_0^1 \text{ such that}\\ a(Tg, v) = b(g, v) \quad \forall\, v \in H_0^1. \end{cases}$$

Operator T is self-adjoint and positive definite with respect to the bilinear forms $a(\cdot,\cdot)$ and $b(\cdot,\cdot)$ on $H^1(\Omega)$, and compact due to the compact embedding of $H^1(\Omega)$ in $L^2(\Omega)$.

Similarly, let $T_h \in \mathcal{L}(L^2(\Omega))$ and $\widetilde{T}_h \in \mathcal{L}(L^2(\Omega))$ be the discrete solution operators associated with the *stabilized* and *nonstabilized* discrete source problems. The former

is the bounded linear operator mapping the forcing term g to $u_h^s =: T_h g$ and satisfies

$$\begin{cases} T_h g \in V_k^h \text{ such that} \\ a_h(T_h g, v_h) = b_h(g, v_h) \quad \forall\, v_h \in V_k^h. \end{cases}$$

The latter is the bounded linear operator mapping the forcing term g to $\widetilde{u}_h^s =: \widetilde{T}_h g$ and satisfies

$$\begin{cases} \widetilde{T}_h g \in V_k^h \text{ such that} \\ a_h(\widetilde{T}_h g, v_h) = \widetilde{b}_h(g, v_h) \quad \forall\, v_h \in V_k^h. \end{cases}$$

Both the operators T_h and $\widetilde{T}_h$ are self-adjoint and positive definite with respect to the discrete bilinear form $a_h(\cdot,\cdot)$, $b_h(\cdot,\cdot)$ and $a_h(\cdot,\cdot)$, $\widetilde{b}_h(\cdot,\cdot)$. They are also compact, since their ranges are finite dimensional.

The eigensolutions of the continuous problem (2.3) and the discrete problems (3.28) and (3.29) are respectively related to the eigenmodes of the operators T, T_h, and $\widetilde{T}_h$. In particular, (λ, u) is an eigenpair of problem (2.3) if and only if $Tu = (1/\lambda)u$, i.e. $(1/\lambda, u)$ is an eigenpair for the operator T, and analogously for problems (3.28) and (3.29) and operators T_h and $\widetilde{T}_h$. Thanks to this correspondence, the convergence analysis can be derived from the spectral approximation theory for compact operators. In the rest of this section we refer only to operators T and $\widetilde{T}_h$. Identical considerations hold for operators T and T_h and we omit them for brevity.

A sufficient condition for the correct spectral approximation of a compact operator T is the uniform convergence of the family of discrete operators $\{\widetilde{T}_h\}_h$ to T (see [27], Proposition 7.4, cf. also [9]):

$$\|T - \widetilde{T}_h\|_{\mathcal{L}(L^2(\Omega))} \to 0 \quad \text{as } h \to 0, \tag{4.1}$$

or, equivalently,

$$\|(T - \widetilde{T}_h)g\|_0 \leqslant C\varrho(h)\|g\|_0 \quad \forall\, g \in L^2(\Omega) \tag{4.2}$$

with $\varrho(h)$ tending to zero as h goes to zero. Condition (4.2) usually follows by a priori estimates with no additional regularity assumption on g. Besides the convergence of the eigenmodes, condition (4.1), or the equivalent condition (4.2), implies that no spurious eigenvalues may pollute the spectrum. In fact, each discrete eigenvalue approximates a continuous eigenvalue and each continuous eigenvalue is approximated by a number of discrete eigenvalues (counted with their multiplicity) that corresponds exactly to its multiplicity.

We now report the main results about the spectral approximation for compact operators (cf. [9], Theorems 7.1–7.4; see also [27], Theorem 9.3–9.7), which deal with the order of convergence of eigenvalues and eigenfunctions.

Theorem 4.1. *Let the uniform convergence* (4.1) *hold true. Let μ be an eigenvalue of T, with multiplicity m, and denote the corresponding eigenspace by E_μ. Then exactly m discrete eigenvalues $\widetilde{\mu}_{1,h}, \dots, \widetilde{\mu}_{m,h}$ (repeated according to their respective multiplicities) converge to μ. Moreover, let $\widetilde{E}_{\mu,h}$ be the direct sum of the eigenspaces corresponding to the discrete eigenvalues $\widetilde{\mu}_{1,h}, \dots, \widetilde{\mu}_{m,h}$ converging to μ. Then*

$$\delta(E_\mu, \widetilde{E}_{\mu,h}) \leqslant C\|(T - \widetilde{T}_h)_{|E_\mu}\|_{\mathcal{L}(L^2(\Omega))}, \tag{4.3}$$

with

$$\delta(E_\mu, \widetilde{E}_{\mu,h}) = \max(\hat{\delta}(E_\mu, \widetilde{E}_{\mu,h}), \hat{\delta}(\widetilde{E}_{\mu,h}, E_\mu)),$$

where, in general,

$$\hat{\delta}(U, W) = \sup_{u \in U, \|u\|_0 = 1} \inf_{w \in W} \|u - w\|_0$$

denotes the gap between subspaces U, $W \subseteq L^2(\Omega)$.

Concerning the eigenvalue approximation error, we recall the following result.

Theorem 4.2. *Let the uniform convergence* (4.1) *hold true. Let $\varphi_1, \dots, \varphi_m$ be a basis of the eigenspace E_μ of T corresponding to the eigenvalue μ, Then, for $i = 1, \dots, m$,*

$$|\mu - \widetilde{\mu}_{i,h}| \leqslant C\bigg(\sum_{j,k=1}^{m} |b((T - \widetilde{T}_h)\varphi_k, \varphi_j)| + \|(T - \widetilde{T}_h)_{|E_\mu}\|^2_{\mathcal{L}(L^2(\Omega))} \bigg), \tag{4.4}$$

where $\widetilde{\mu}_{1,h}, \dots, \widetilde{\mu}_{m,h}$ are the m discrete eigenvalues converging to μ repeated according to their multiplicities.

4.2. Convergence analysis for the stabilized formulation. In this section we study the convergence of the discrete eigenmodes provided by the VEM approximation to the continuous ones. We will consider the stabilized discrete formulation (3.29). The analysis can be easily applied to the nonstabilized one (3.28).

Theorem 4.3. *The family of operators $\widetilde{T}_h$ converges uniformly to the operator T, that is,*

$$\|T - \widetilde{T}_h\|_{\mathcal{L}(L^2(\Omega))} \to 0 \quad \text{for} \quad h \to 0. \tag{4.5}$$

P r o o f. The proof follows the same lines as those of Theorem 6.4 in [40]. We recall it here for the convenience of the reader. Let u^s and $\tilde{u}_h^s$ be the solutions to the continuous and the discrete source problems (2.6) and (3.30), respectively. From the L^2-estimate of Theorem 3.3 with $g \in L^2(\Omega)$ and the stability estimate in (2.7) we have that

$$\|u^s - \tilde{u}_h^s\|_0 \leqslant Ch^{\min(t+1,1)}\|g\|_0$$

with $t = \min(k, r)$, $k \geqslant 1$ being the order of the method and r the regularity index of the solution $u^s \in H^{1+r}(\Omega)$ to the continuous source problem. Then it follows that

$$\|T - \widetilde{T}_h\|_{\mathcal{L}(L^2(\Omega))} = \sup_{g\in L^2(\Omega)} \frac{\|Tg - \widetilde{T}_h g\|_0}{\|g\|_0} = \sup_{g\in L^2(\Omega)} \frac{\|u^s - \tilde{u}_h^s\|_0}{\|g\|_0} \leqslant Ch^{\min(t+1,1)}.$$

□

We note that if $g \in \mathcal{E}_\mu$ then, thanks to the L^2 a priori error estimate in Remark 3.4, we have

$$\|(T - \widetilde{T}_h)_{|E_\mu}\|_{\mathcal{L}(L^2(\Omega))} = \sup_{g\in\mathcal{E}_\mu} \frac{\|Tg - \widetilde{T}_h g\|_0}{\|g\|_0} = \sup_{g\in\mathcal{E}_\mu} \frac{\|u^s - \tilde{u}_h^s\|_0}{\|g\|_0} \leqslant Ch^{t+1}.$$

Putting together Theorem 4.1, Theorem 4.3, and the above observation, we can state the following result.

Theorem 4.4. *Let μ be an eigenvalue of T, with multiplicity m, and denote the corresponding eigenspace by E_μ. Then exactly m discrete eigenvalues $\widetilde{\mu}_{1,h}, \ldots, \widetilde{\mu}_{m,h}$ (repeated according to their respective multiplicities) converge to μ. Moreover, let $\widetilde{E}_{\mu,h}$ be the direct sum of the eigenspaces corresponding to the discrete eigenvalues $\widetilde{\mu}_{1,h}, \ldots, \widetilde{\mu}_{m,h}$ converging to μ. Then*

$$\delta(E_\mu, \widetilde{E}_{\mu,h}) \leqslant Ch^{t+1}. \tag{4.6}$$

A direct consequence of the previous result (cf. [9], [27]) is the following one.

Theorem 4.5. *Let u be a unit eigenfunction associated with the eigenvalue λ of multiplicity m and let $\widetilde{w}_h^{(1)}, \ldots, \widetilde{w}_h^{(m)}$ denote linearly independent eigenfunctions associated with the m discrete eigenvalues of problem (3.29) converging to λ. Then there exists $\widetilde{u}_h \in \operatorname{span}\{\widetilde{w}_h^{(1)}, \ldots, \widetilde{w}_h^{(m)}\}$ such that*

$$\|u - \widetilde{u}_h\|_0 \leqslant Ch^{t+1},$$

where $t = \min\{k, r\}$, k being the order of the method, and r the regularity index of u.

We now state the usual double order convergence of the eigenvalues.

Theorem 4.6. *Let λ be an eigenvalue of problem* (2.3) *with multiplicity m, and denote by $\widetilde{\lambda}_{1,h}, \ldots, \widetilde{\lambda}_{m,h}$ the m discrete eigenvalues of problem* (3.29) *converging towards λ. Then the following optimal double order convergence holds:*

$$|\lambda - \widetilde{\lambda}_{i,h}| \leqslant Ch^{2t} \quad \forall\, i = 1, \ldots, m, \tag{4.7}$$

with $t = \min\{k, r\}$, k being the order of the method, and r the regularity index of the eigenfunction corresponding to λ.

P r o o f. The proof follows the guidelines of Theorem 6.4 in [40] and Theorems 4.2 and 4.3 in [48]. For an alternative proof see also Theorem 6.6. in [39], taking into account that in our case the term $\mathcal{N}_h(\cdot, \cdot)$, relative to the *conformity* error, vanishes. □

Eventually, we state the optimal error estimate for the eigenfunctions in the energy norm.

Theorem 4.7. *With the same notation as in Theorem* 4.5, *we have*

$$|u - \widetilde{u}_h|_1 \leqslant Ch^t,$$

where $t = \min(k, r)$, k being the order of the method, and r the regularity index of $u \in H^{1+r}(\Omega)$.

P r o o f. The proof of this result is similar to the one for the finite element method. We briefly report it here for the sake of completeness. It holds that

$$u - \widetilde{u}_h = \lambda T u - \widetilde{\lambda}_h \widetilde{T}_h \widetilde{u}_h = (\lambda - \widetilde{\lambda}_h) T u + \widetilde{\lambda}_h (T - \widetilde{T}_h) u + \widetilde{\lambda}_h \widetilde{T}_h (u - \widetilde{u}_h),$$

then

$$|u - \widetilde{u}_h|_1 \leqslant |\lambda - \widetilde{\lambda}_h|\, |Tu|_1 + \widetilde{\lambda}_h |(T - \widetilde{T}_h) u|_1 + \widetilde{\lambda}_h |\widetilde{T}_h (u - \widetilde{u}_h)|_1.$$

The first term on the right-hand side of the previous equation is of order h^{2t}, while the second is of order h^t. Finally, for the last term, using (3.23), the continuity of the operator $\widetilde{T}_h$, and Theorem 4.5, we obtain

$$\begin{aligned} |\widetilde{T}_h (u - \widetilde{u}_h)|_1^2 &\leqslant \frac{1}{\alpha_*} a_h (\widetilde{T}_h (u - \widetilde{u}_h), \widetilde{T}_h (u - \widetilde{u}_h)) \\ &= \frac{1}{\alpha_*} \widetilde{b}_h (u - \widetilde{u}_h, \widetilde{T}_h (u - \widetilde{u}_h)) \leqslant C \|u - \widetilde{u}_h\|_0^2 \leqslant Ch^{2t+2}. \end{aligned}$$

□

5. Numerical experiments

In this section, we investigate the behavior of the virtual element method for the numerical treatment of the eigenvalue problem (2.3). In particular, we present the performance of the conforming VEM applied to the eigenvalue problem on a two-dimensional square domain. We use the "diagonal" stabilization [14] for the bilinear form $a_h^P(\cdot,\cdot)$ (cf. (3.20)) and $\widetilde{b}_h^P(\cdot,\cdot)$ (cf. (3.27)), which reads as follows:

$$S^P(v_h, w_h) = \sigma_P \mathbf{v}_h^{\mathrm{T}} \mathbf{w}_h,$$
$$\widetilde{S}^P(v_h, w_h) = \tau_P h_P^2 \mathbf{v}_h^{\mathrm{T}} \mathbf{w}_h,$$

where $\mathbf{v}_h$, $\mathbf{w}_h$ denote the vectors containing the values of the local degrees of freedom associated to $v_h, w_h \in V_k^h(P)$ and the parameters σ_P and τ_P are two positive h-independent constants. In the numerical tests we choose σ_P as the mean value of the eigenvalues of the matrix stemming from the consistency term $(\Pi_{k-1}^{0,P}\nabla\cdot, \Pi_{k-1}^{0,P}\nabla\cdot)_P$ for the grad-grad form (see (3.20)). In the same way we pick τ_P as the mean value of the eigenvalues of the matrix resulting from the term $h_P^{-2}(\Pi_k^{0,P}\cdot, \Pi_k^{0,P}\cdot)_P$ for the mass matrix (see (3.27)).

The convergence of the numerical approximation is shown through the relative error quantity

$$\textit{Relative approximation error} := \frac{|\lambda - \lambda_h|}{\lambda},$$

where λ denotes an eigenvalue of the continuous problem and λ_h its virtual element approximation. In all figures of this section, the approximation errors are displayed in log-log plots where the convergence rate is reflected by the slope of the corresponding error curve. The x-axis is reversed to show decreasing errors curves towards the right.

5.1. Test 1 (quantum harmonic oscillator). In this test case, we numerically solve the 2D quantum harmonic oscillator problem that corresponds to the Schrödinger equation with the harmonic potential $V(x,y) = \frac{1}{2}(x^2+y^2)$. The eigenvalues are suitable combinations of the eigenvalues of the one dimensional problem and are given by the natural numbers $n = 1, 2, 3, \ldots$, each one with multiplicity n. The eigenfunctions of such a problem are obtained through the two-dimensional tensor product of one-dimensional Hermite functions, which are given by the Hermite polynomials multiplied by the Gaussian function $w(x,y) = \exp\bigl(-(x^2+y^2)\bigr)$. As these eigenfunctions are rapidly decreasing to zero for x, y tending to infinity due to the Gaussian term, we can assume homogeneous Dirichlet boundary conditions if the computational domain is sufficiently large. For such reason, we solve the eigenvalue problem on the square domain $\Omega =]-10, 10[\times]-10, 10[$. On this domain, we consider four different mesh sequences, hereafter denoted by:

▷ *Mesh 1*, mainly hexagonal mesh with continuously distorted cells,
▷ *Mesh 2*, nonconvex octagonal mesh,
▷ *Mesh 3*, randomized quadrilateral mesh,
▷ *Mesh 4*, central Voronoi tessellation.

The first mesh of each sequence is shown in Figure 1. These mesh sequences have been widely used in the mimetic finite difference and virtual element literature, and a detailed description of their construction can easily be found elsewhere, for example, see [18].

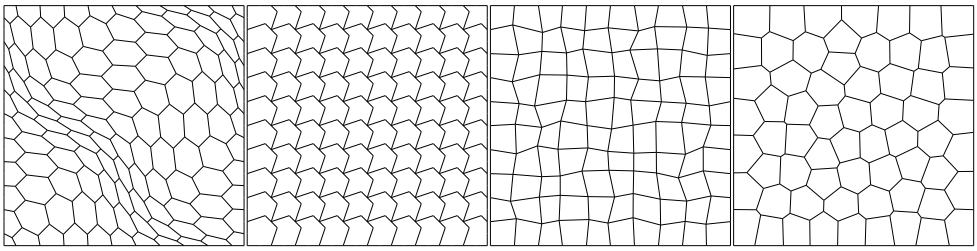

Figure 1. Base meshes of the following mesh families from left to right: mainly hexagonal mesh; nonconvex octagonal mesh; randomized quadrilateral mesh; Voronoi mesh.

The convergence curves for the four mesh sequences above are reported in Figures 2, 3, 4, and 5 (notice that the mesh sizes h are displayed in the decreasing order).

The expected rate of convergence is shown in each panel by the triangle closed to the error curve and indicated by an explicit label.

For these calculations, we used the VEM approximation based on the conforming virtual element space V_k^h, $k = 1, 2, 3, 4$, and the VEM formulation (3.28) using the nonstabilized bilinear form $b_h(\cdot, \cdot)$. As already observed in [40] for the conforming VEM approximation of the Laplace eigenvalue problem, the same computations using formulation (3.29) and the stabilized bilinear $\widetilde{b}_h(\cdot, \cdot)$ produce almost identical results, which, for this reason, are not shown here. These plots confirm that the conforming VEM formulations proposed in this work provide a numerical approximation with optimal convergence rate on a set of representative mesh sequences, including deformed and nonconvex cells, of the Schrödinger equation problem, i.e., the standard eigenvalue problem with a regular potential term in the Hamilton operator at the left hand-side.

5.2. Test 2 (piecewise constant diffusivity tensor). The present test problem is taken from the benchmark singular solution set in [37]. We here consider the square domain $\Omega = (-1, 1)^2$ split into two subdomains Ω_δ and Ω_1 (see the left plot

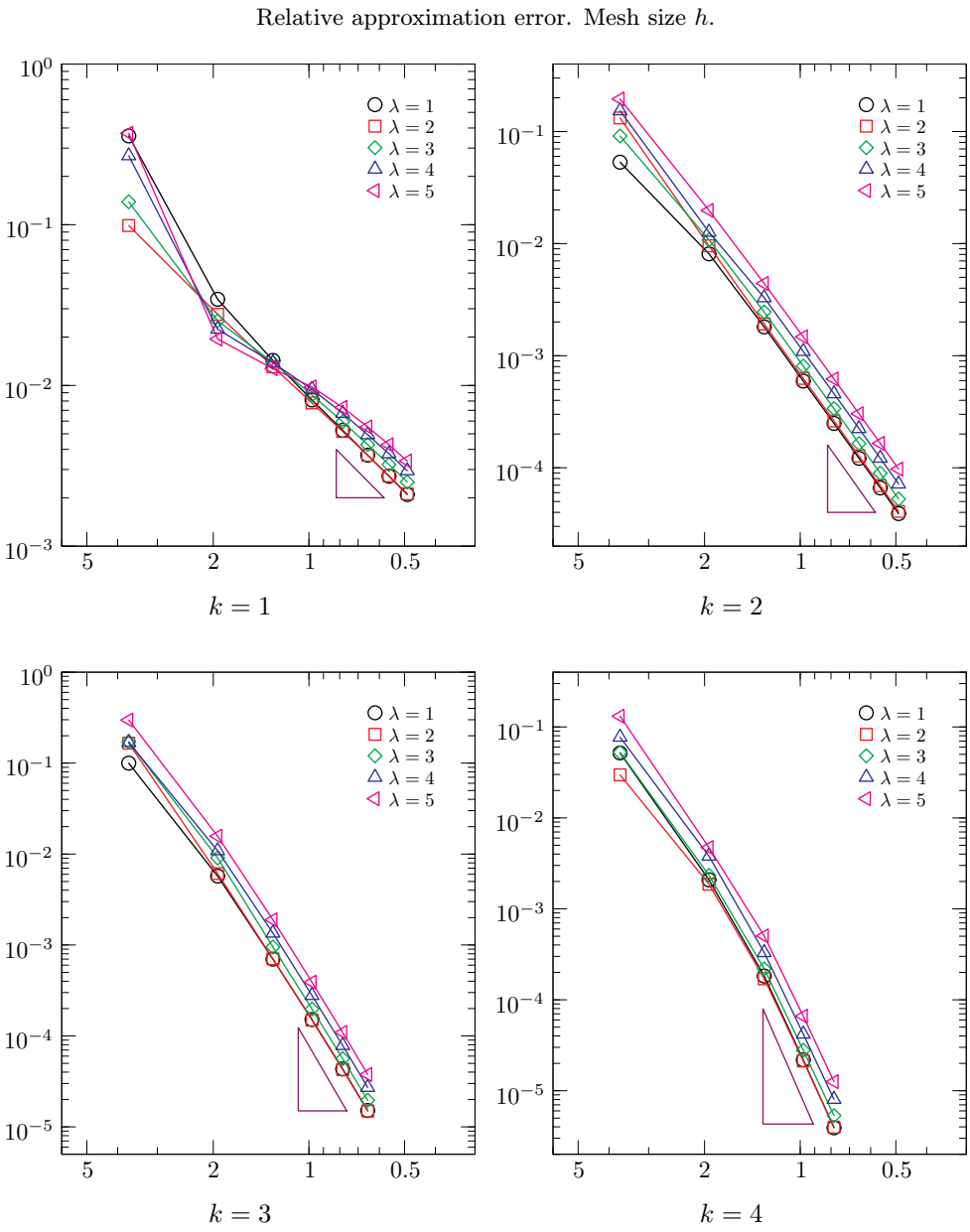

Figure 2. Test Case 1: Convergence plots for the approximation of the first five distinct eigenvalues $\lambda = 1, 2, 3, 4, 5$ using the mainly hexagonal mesh and the virtual spaces V_k^h with $k = 1$ (top-leftmost panel), $k = 2$ (top-rightmost panel), $k = 3$ (bottom-leftmost panel), $k = 4$ (bottom-rightmost panel). The generalized eigenvalue problem uses the nonstabilized bilinear form $b_h(\cdot, \cdot)$.

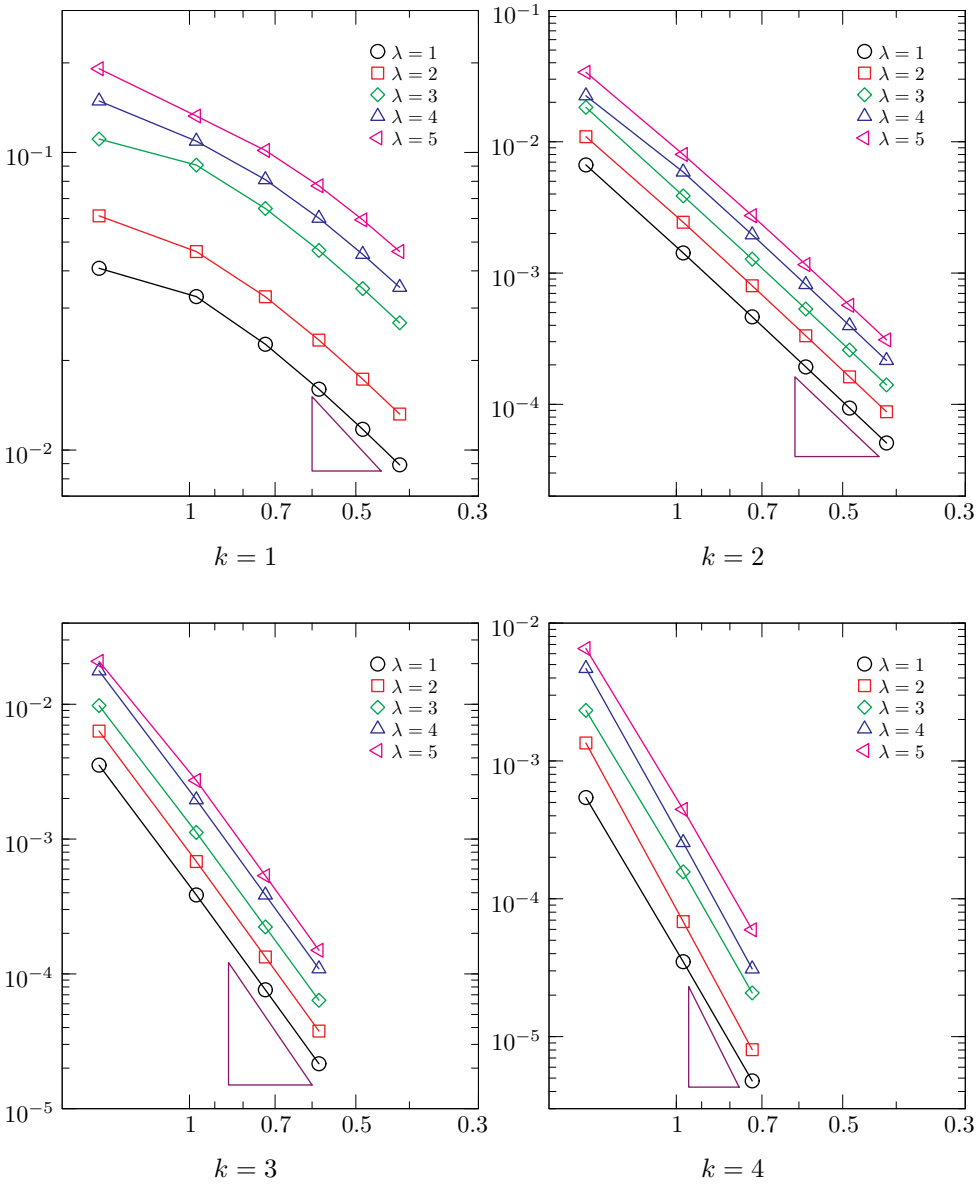

Figure 3. Test Case 1: Convergence plots for the approximation of the first five distinct eigenvalues $\lambda = 1, 2, 3, 4, 5$ using the nonconvex octagonal mesh and the virtual spaces V_k^h with $k = 1$ (top-leftmost panel), $k = 2$ (top-rightmost panel), $k = 3$ (bottom-leftmost panel), $k = 4$ (bottom-rightmost panel). The generalized eigenvalue problem uses the nonstabilized bilinear form $b_h(\cdot, \cdot)$.

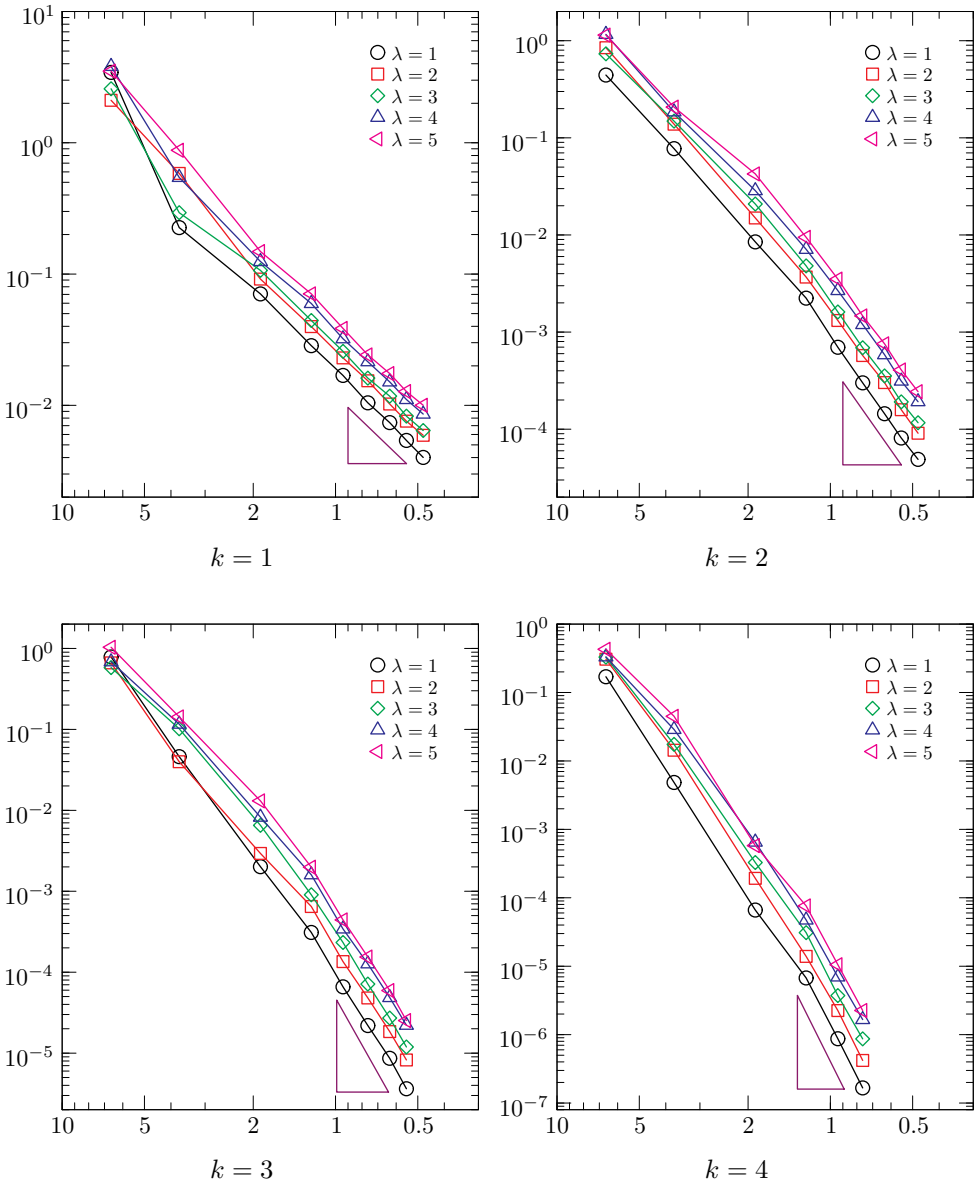

Figure 4. Test Case 1: Convergence plots for the approximation of the first five distinct eigenvalues $\lambda = 1, 2, 3, 4, 5$ using the randomized quadrilateral mesh and the virtual spaces V_k^h with $k = 1$ (top-leftmost panel), $k = 2$ (top-rightmost panel), $k = 3$ (bottom-leftmost panel), $k = 4$ (bottom-rightmost panel). The generalized eigenvalue problem uses the nonstabilized bilinear form $b_h(\cdot, \cdot)$.

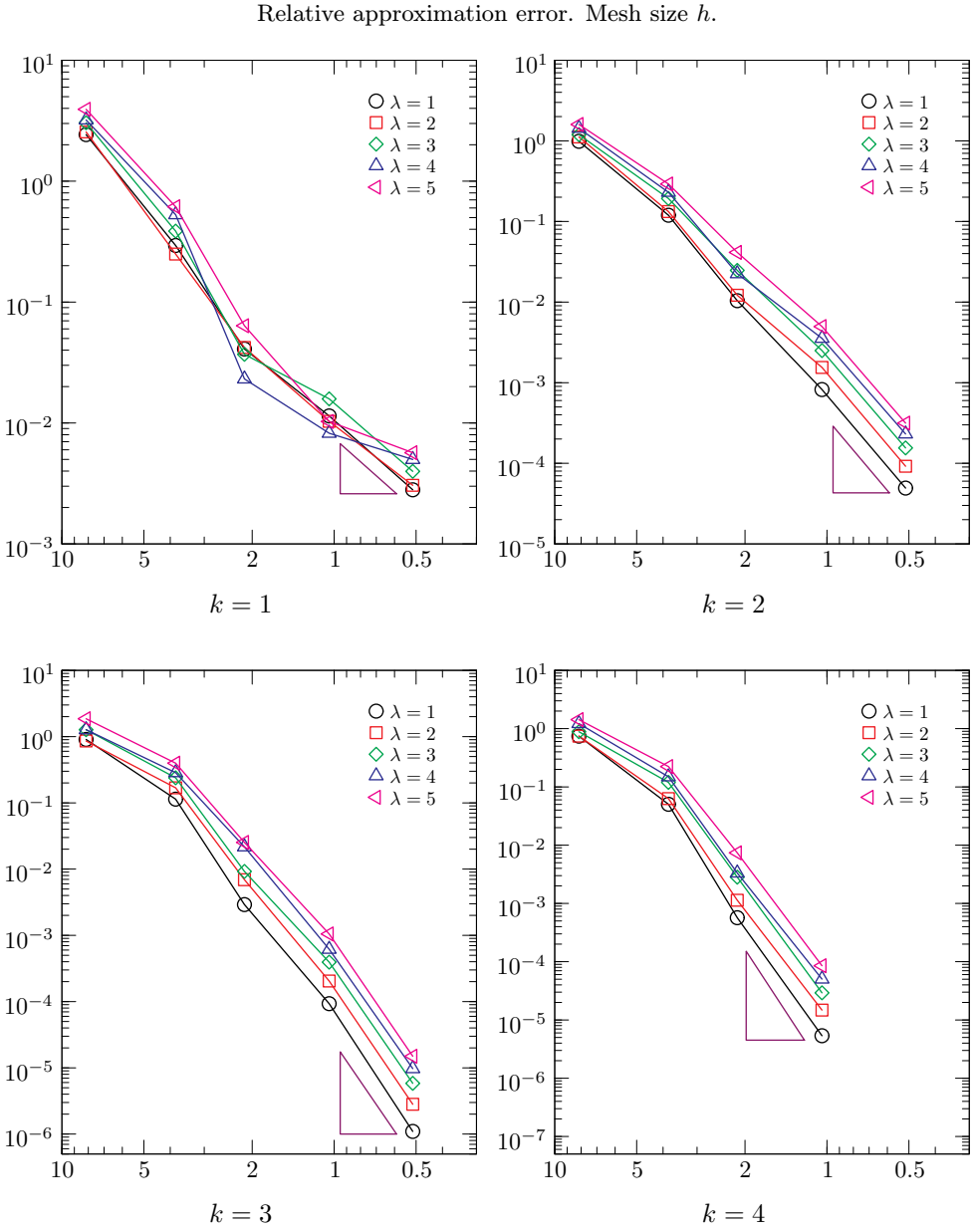

Figure 5. Test Case 1: Convergence plots for the approximation of the first five distinct eigenvalues $\lambda = 1, 2, 3, 4, 5$ using the Voronoi mesh and the virtual spaces V_k^h with $k = 1$ (top-leftmost panel), $k = 2$ (top-rightmost panel), $k = 3$ (bottom-leftmost panel), $k = 4$ (bottom-rightmost panel). The generalized eigenvalue problem uses the nonstabilized form $b_h(\cdot, \cdot)$.

in Figure 6), and we study the eigenvalue problem on the square with discontinuous diffusivity tensor and zero potential V coupled with Neumann homogeneous boundary conditions, i.e. we consider the following problem in strong form:

$$-\nabla \cdot (\mathbb{K}(\mathbf{x})\nabla u(\mathbf{x})) = \lambda u(\mathbf{x}) \quad \text{in } \Omega \quad \text{and} \quad \frac{\partial u}{\partial n} = 0 \quad \text{on } \Gamma.$$

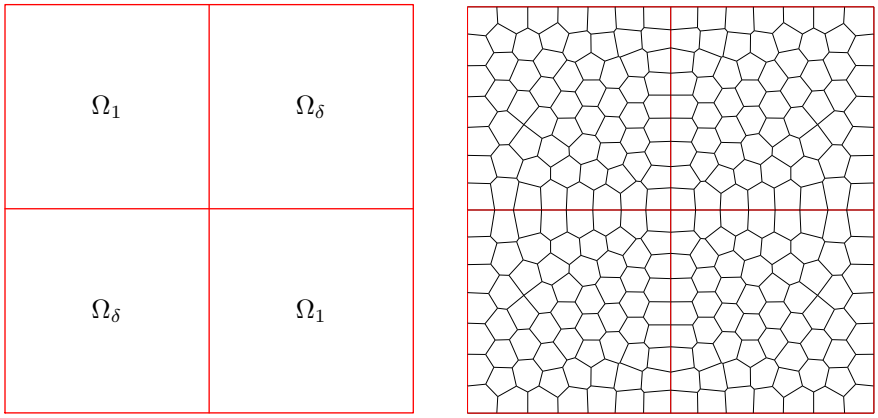

Figure 6. Test Case 2: Left plot: subdivision of Ω into the subdomains Ω_δ and Ω_1. Right plot: Example of locally Voronoi decomposition of Ω.

Therefore, the continuous bilinear form associated to the eigenvalue problem is

$$a_{\mathbb{K}}^P(u,v) := \int_P \mathbb{K}\nabla u \cdot \nabla v \, \mathrm{d}\mathbf{x},$$

whose virtual approximation (see [13], [15]) is given by

$$a_{h,\mathbb{K}}^P(u_h,v_h) = \int_P \mathbb{K}\Pi_{k-1}^{0,P}\nabla u_h \cdot \Pi_{k-1}^{0,P}\nabla v_h \, \mathrm{d}\mathbf{x} + \overline{\mathbb{K}} S^P((I-\Pi_k^{\nabla,P})u_h, (I-\Pi_k^{\nabla},P)v_h) \tag{5.1}$$

to be used in place of $a_h^P(u_h,v_h)$ (cf. (3.20)) in problem (3.29), where $\overline{\mathbb{K}} = \|\mathbb{K}\|_{\infty,P}$. We consider $\mathbb{K}_{|\Omega_1} = I$ and $\mathbb{K}_{|\Omega_\delta} = \delta^{-1}I$ with four different values of δ, namely $\delta = 0.50, 0.10, 0.01, 1e-8$.

We apply the Virtual Element method (3.29) using a sequence of Voronoi meshes with mesh diameters $h = \frac{1}{2}, \frac{1}{4}, \frac{1}{8}, \frac{1}{16}$ (see the right plot in Figure 6 for an example of the adopted meshes). We show the plot of the convergence for the first eight

computed eigenvalues in Figures 7, 8, 9, 10. We compute the relative errors by comparing our results with the values given in [37].

In accordance with Theorem 4.6, we obtain different rates of convergence that are determined by the polynomial order of the method and by the regularity of the corresponding exact eigenfunctions [37]. For instance, the order of convergence for almost all the eigenvalues relative to $\delta = 0.50$, for the second and sixth eigenvalue relative to $\delta = 0.10$ and for the third and the seventh eigenvalue relative to $\delta = 0.01$ are determined by the regularity index of the corresponding eigenfunction. We notice also that the convergence curve for the second eigenvalue relative to $\delta = 10^{-8}$ has a big jump up on the finest mesh for $k = 3$. This phenomena could be due to the fact that, in this case, the reference solution from Dauge's benchmark is correct up to six digits. Taking this into account, we show that the method is overall optimal, and thus stable with respect to discontinuities in the diffusivity tensor.

6. Conclusions

We have discussed the application of the conforming virtual element method to the numerical resolution of eigenvalue problems with potential terms on polytopic meshes. The most notable case is that of the Schrödinger equation with a suitable pseudopotential, which is fundamental in the numerical treatment of more complex problems in the Density Functional Theory. The VEM approximation of such problem was discussed from both the theoretical and the numerical viewpoint, proving that the method provides a correct spectral approximation with optimal rates of convergence. The performance of the method was shown by computing the first eigenvalues of the quantum harmonic oscillator provided by the harmonic potential and a singular eigenvalue problem with zero potential.

References

[1] *R. A. Adams*: Sobolev Spaces. Pure and Applied Mathematics 65, Academic Press, New York, 1975. zbl MR

[2] *S. Agmon*: Lectures on Elliptic Boundary Value Problems. Van Nostrand Mathematical Studies 2, Princeton, Toronto, 1965. zbl MR

[3] *B. Ahmad, A. Alsaedi, F. Brezzi, L. D. Marini, A. Russo*: Equivalent projectors for virtual element methods. Comput. Math. Appl. *66* (2013), 376–391. zbl MR doi

[4] *P. F. Antonietti, L. Beirão da Veiga, S. Scacchi, M. Verani*: A C^1 virtual element method for the Cahn-Hilliard equation with polygonal meshes. SIAM J. Numer. Anal. *54* (2016), 34–56. zbl MR doi

[5] *P. F. Antonietti, G. Manzini, M. Verani*: The fully nonconforming virtual element method for biharmonic problems. Math. Models Methods Appl. Sci. *28* (2018), 387–407. zbl MR doi

[6] *P. F. Antonietti, L. Mascotto, M. Verani*: A multigrid algorithm for the p-version of the virtual element method. ESAIM, Math. Model. Numer. Anal. *52* (2018), 337–364. doi

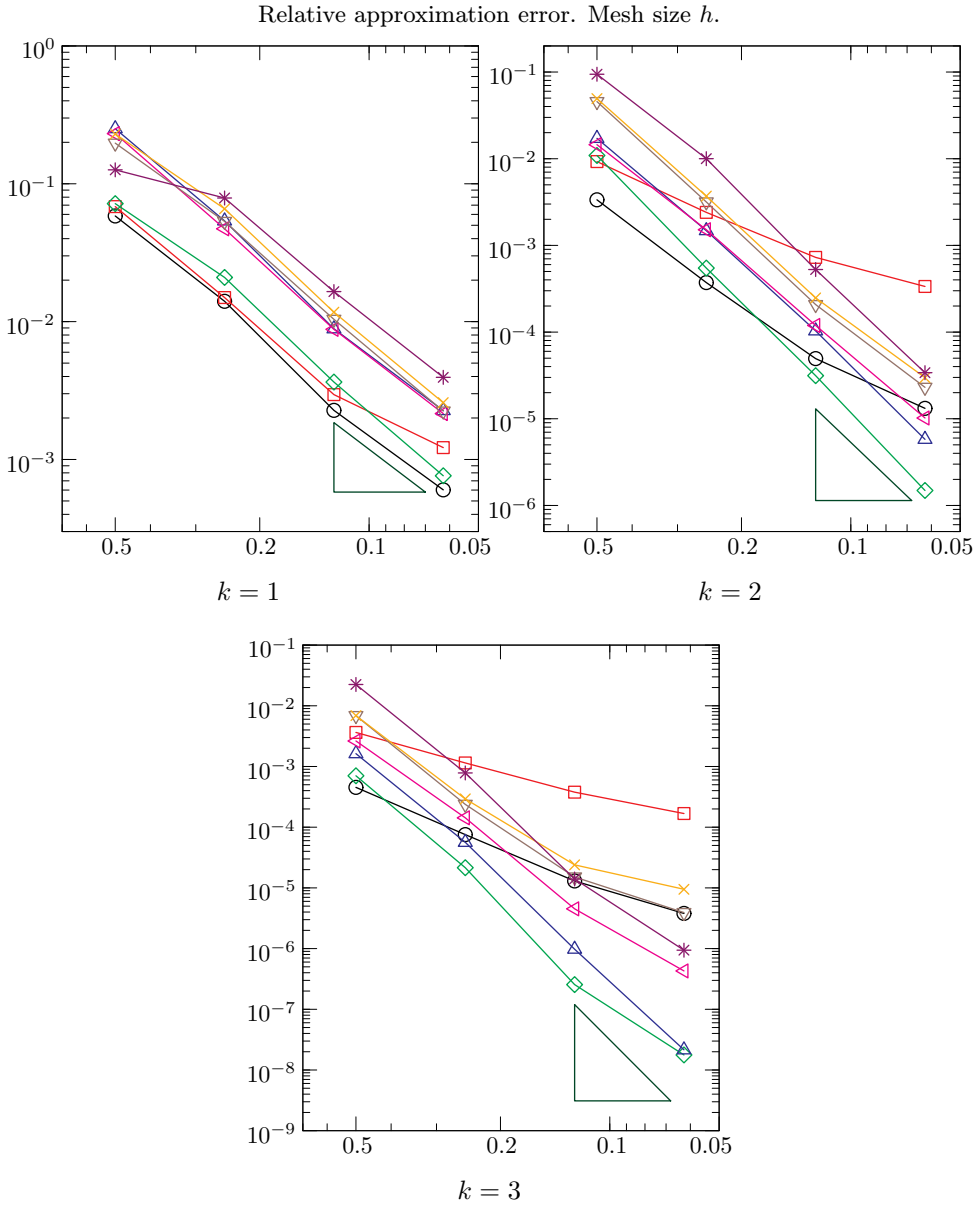

Figure 7. Discontinuous diffusion problem, $\delta = 0.50$; the symbols that label the eigenvalues are in the following order: circle, square, diamond, triangle up, triangle left, triangle down, cross, star. The generalized eigenvalue problem uses the stabilized bilinear form $\widetilde{b}_h(\cdot, \cdot)$.

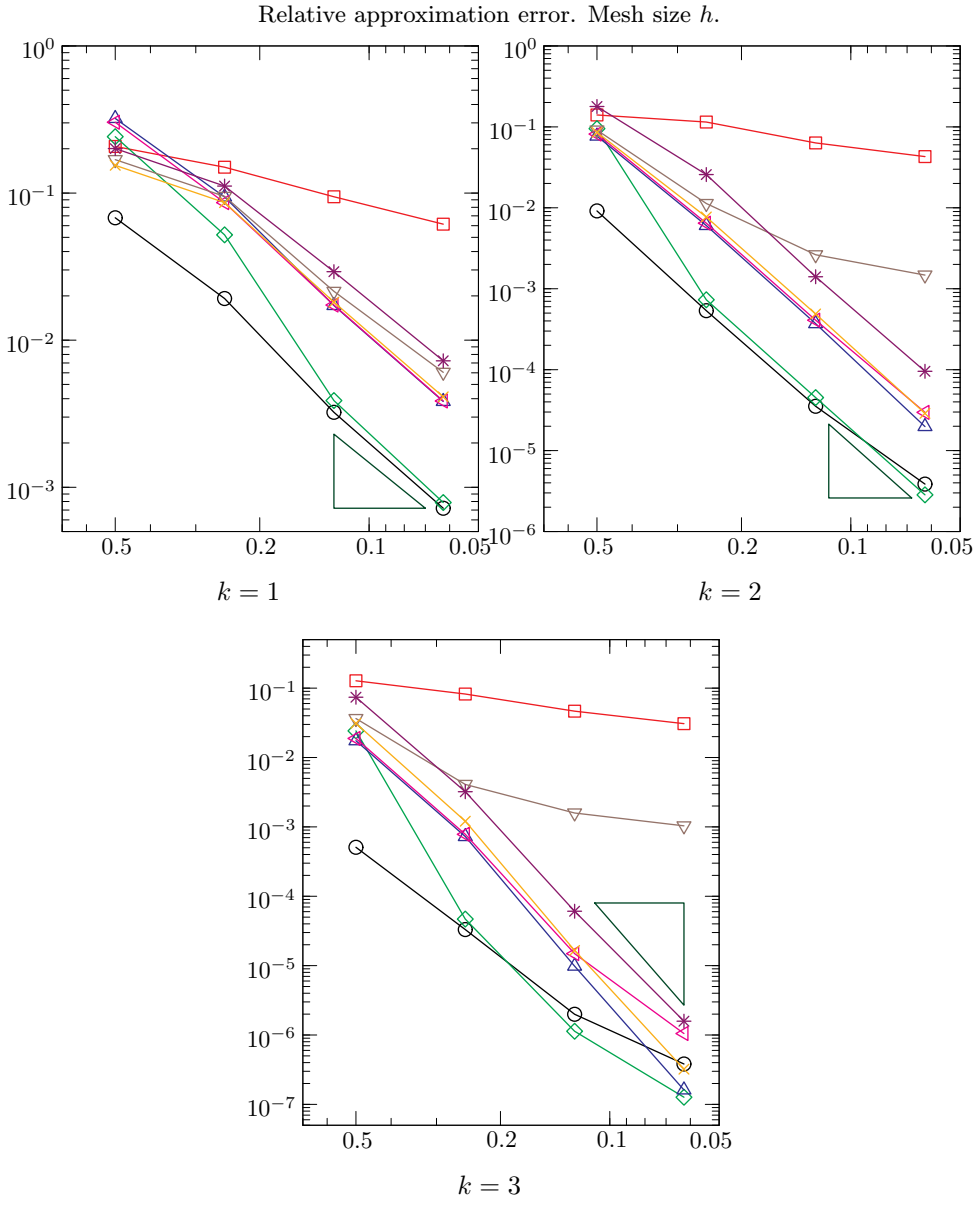

Figure 8. Discontinuous diffusion problem, $\delta = 0.10$; the symbols that label the eigenvalues are in the following order: circle, square, diamond, triangle up, triangle left, triangle down, cross, star. The generalized eigenvalue problem uses the stabilized bilinear form $\widetilde{b}_h(\cdot, \cdot)$.

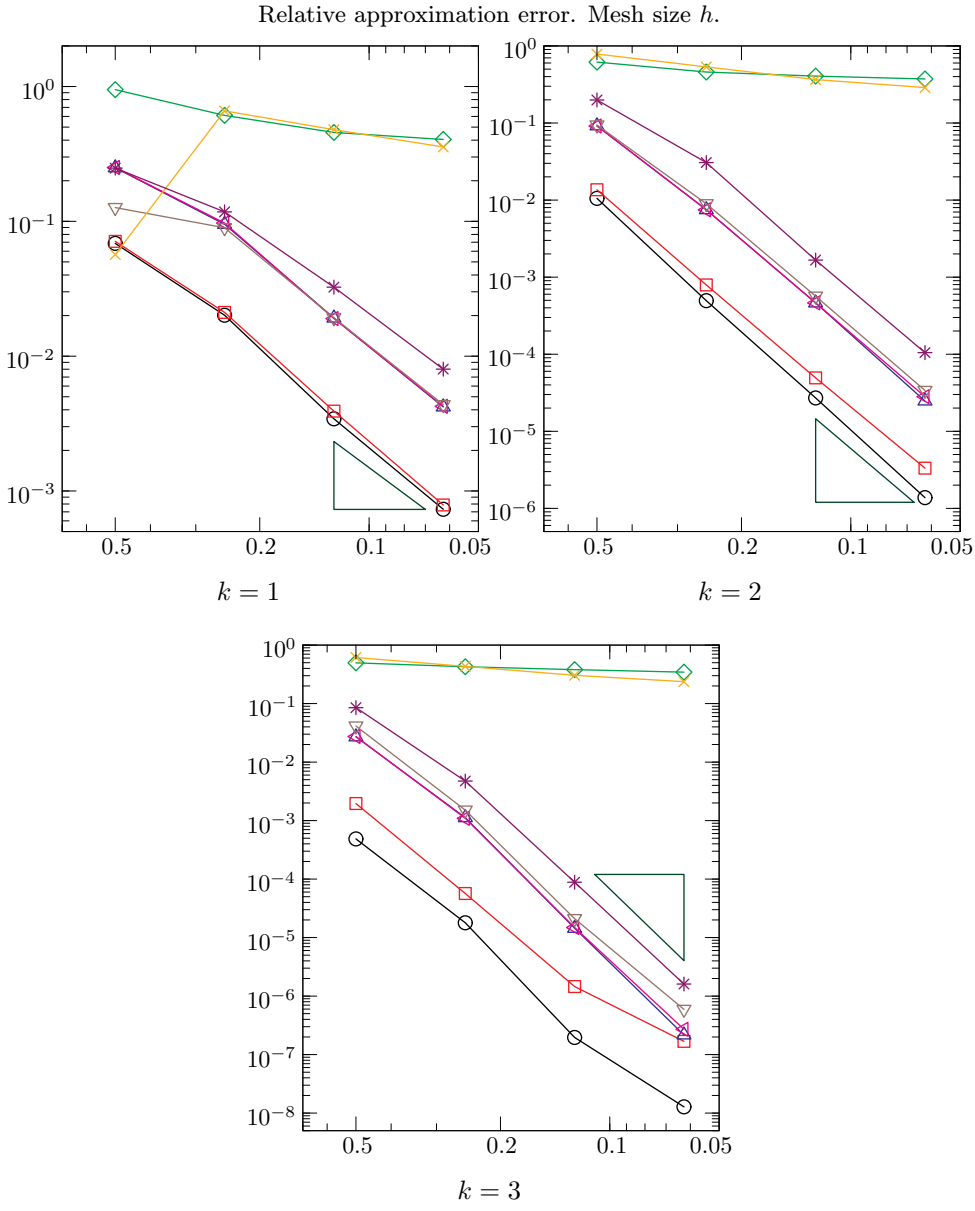

Figure 9. Discontinuous diffusion problem, $\delta = 0.01$; the symbols that label the eigenvalues are in the following order: circle, square, triangle left, triangle down, cross, star. The generalized eigenvalue problem uses the stabilized form $\widetilde{b}_h(\cdot, \cdot)$.

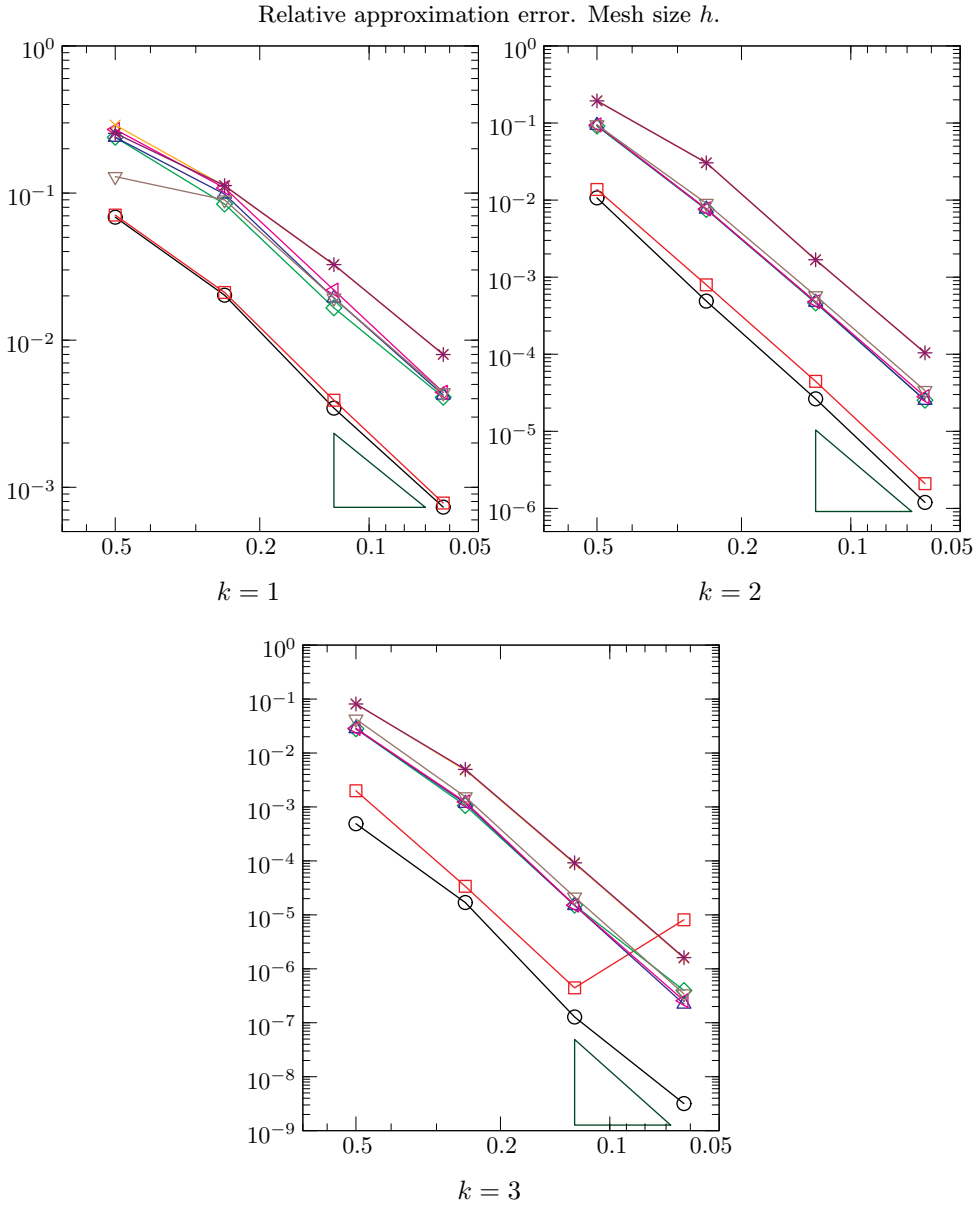

Figure 10. Discontinuous diffusion problem, $\delta = 10^{-8}$; the symbols that label the eigenvalues are in the following order: circle, square, diamond, triangle up, triangle left, triangle down, cross, star. The generalized eigenvalue problem uses the stabilized bilinear form $\widetilde{b}_h(\cdot,\cdot)$.

[7] *E. Artioli, S. De Miranda, C. Lovadina, L. Patruno*: A stress/displacement Virtual Element method for plane elasticity problems. Comput. Meth. Appl. Mech. Eng. *325* (2017), 155–174. MR doi

[8] *B. Ayuso de Dios, K. Lipnikov, G. Manzini*: The nonconforming virtual element method. ESAIM, Math. Model. Numer. Anal. *50* (2016), 879–904. zbl MR doi

[9] *I. Babuška, J. Osborn*: Eigenvalue problems. Handbook of Numerical Analysis. Volume II: Finite Element Methods (Part 1) (P. G. Ciarlet, ed.). North-Holland, Amsterdam, 1991, pp. 641–787. zbl MR doi

[10] *R. F. W. Bader*: A quantum theory of molecular structure and its applications. Chem. Rev. *91* (1991), 893–928. doi

[11] *L. Beirão da Veiga, F. Brezzi, A. Cangiani, G. Manzini, L. D. Marini, A. Russo*: Basic principles of virtual element methods. Math. Models Methods Appl. Sci. *23* (2013), 199–214. zbl MR doi

[12] *L. Beirão da Veiga, F. Brezzi, F. Dassi, L. D. Marini, A. Russo*: Virtual element approximation of 2D magnetostatic problems. Comput. Methods Appl. Mech. Eng. *327* (2017), 173–195. MR doi

[13] *L. Beirão da Veiga, F. Brezzi, F. Dassi, L. D. Marini, A. Russo*: Serendipity virtual elements for general elliptic equations in three dimensions. Chin. Ann. Math., Ser. B *39* (2018), 315–334. zbl MR doi

[14] *L. Beirão da Veiga, F. Brezzi, L. D. Marini, A. Russo*: The Hitchhiker's guide to the virtual element method. Math. Models Methods Appl. Sci. *24* (2014), 1541–1573. zbl MR doi

[15] *L. Beirão da Veiga, F. Brezzi, L. D. Marini, A. Russo*: Virtual element method for general second-order elliptic problems on polygonal meshes. Math. Models Methods Appl. Sci. *26* (2016), 729–750. zbl MR doi

[16] *L. Beirão da Veiga, A. Chernov, L. Mascotto, A. Russo*: Basic principles of *hp* virtual elements on quasiuniform meshes. Math. Models Methods Appl. Sci. *26* (2016), 1567–1598. zbl MR doi

[17] *L. Beirão da Veiga, F. Dassi, A. Russo*: High-order virtual element method on polyhedral meshes. Comput. Math. Appl. *74* (2017), 1110–1122. zbl MR doi

[18] *L. Beirão da Veiga, K. Lipnikov, G. Manzini*: Arbitrary-order nodal mimetic discretizations of elliptic problems on polygonal meshes. SIAM J. Numer. Anal. *49* (2011), 1737–1760. zbl MR doi

[19] *L. Beirão da Veiga, K. Lipnikov, G. Manzini*: The Mimetic Finite Difference Method for Elliptic Problems. MS&A. Modeling, Simulation and Applications 11, Springer, Cham, 2014. zbl MR doi

[20] *L. Beirão da Veiga, C. Lovadina, G. Vacca*: Divergence free virtual elements for the Stokes problem on polygonal meshes. ESAIM, Math. Model. Numer. Anal. *51* (2017), 509–535. zbl MR doi

[21] *L. Beirão da Veiga, C. Lovadina, G. Vacca*: Virtual elements for the Navier-Stokes problem on polygonal meshes. SIAM J. Numer. Anal. *56* (2018), 1210–1242. zbl MR doi

[22] *L. Beirão da Veiga, G. Manzini*: A virtual element method with arbitrary regularity. IMA J. Numer. Anal. *34* (2014), 759–781. zbl MR doi

[23] *L. Beirão da Veiga, G. Manzini*: Residual a posteriori error estimation for the virtual element method for elliptic problems. ESAIM, Math. Model. Numer. Anal. *49* (2015), 577–599. zbl MR doi

[24] *L. Beirão da Veiga, D. Mora, G. Rivera, R. Rodríguez*: A virtual element method for the acoustic vibration problem. Numer. Math. *136* (2017), 725–763. zbl MR doi

[25] *L. Beirão da Veiga, A. Russo, G. Vacca*: The virtual element method with curved edges. Available at `https://arxiv.org/abs/1711.04306` (2017), 29 pages.

[26] *M. F. Benedetto, S. Berrone, A. Borio, S. Pieraccini, S. Scialò*: A hybrid mortar virtual element method for discrete fracture network simulations. J. Comput. Phys. *306* (2016), 148–166. zbl MR doi
[27] *D. Boffi*: Finite element approximation of eigenvalue problems. Acta Numerica *19* (2010), 1–120. zbl MR doi
[28] *F. Brezzi, L. D. Marini*: Virtual element methods for plate bending problems. Comput. Methods Appl. Mech. Eng. *253* (2013), 455–462. zbl MR doi
[29] *E. Cáceres, G. N. Gatica*: A mixed virtual element method for the pseudostress-velocity formulation of the Stokes problem. IMA J. Numer. Anal. *37* (2017), 296–331. MR doi
[30] *Y. Cai, Z. Bai, J. E. Pask, N. Sukumar*: Hybrid preconditioning for iterative diagonalization of ill-conditioned generalized eigenvalue problems in electronic structure calculations. J. Comput. Phys. *255* (2013), 16–30. zbl MR doi
[31] *A. Cangiani, F. Gardini, G. Manzini*: Convergence of the mimetic finite difference method for eigenvalue problems in mixed form. Comput. Methods Appl. Mech. Eng. *200* (2011), 1150–1160. zbl MR doi
[32] *A. Cangiani, V. Gyrya, G. Manzini*: The nonconforming virtual element method for the Stokes equations. SIAM J. Numer. Anal. *54* (2016), 3411–3435. zbl MR doi
[33] *A. Cangiani, G. Manzini, A. Russo, N. Sukumar*: Hourglass stabilization and the virtual element method. Int. J. Numer. Meth. Eng. *102* (2015), 404–436. zbl MR doi
[34] *A. Cangiani, G. Manzini, O. Sutton*: Conforming and nonconforming virtual element methods for elliptic problems. IMA J. Numer. Anal. Analysis *37* (2017), 1317–1354. MR doi
[35] *H. Chi, L. Beirão da Veiga, G. H. Paulino*: Some basic formulations of the virtual element method (VEM) for finite deformations. Comput. Methods Appl. Mech. Eng. *318* (2017), 148–192. MR doi
[36] *F. Dassi, L. Mascotto*: Exploring high-order three dimensional virtual elements: bases and stabilizations. Comput. Math. Appl. *75* (2018), 3379–3401. MR doi
[37] *M. Dauge*: Benchmark computations for Maxwell equations for the approximation of highly singular solutions. Available at `https://perso.univ-rennes1.fr/monique.dauge/benchmax.html` (2004).
[38] *A. Ern, J. L. Guermond*: Theory and Practice of Finite Elements. Applied Mathematical Sciences 159, Springer, New York, 2004. zbl MR doi
[39] *F. Gardini, G. Manzini, G. Vacca*: The nonconforming virtual element method for eigenvalue problems. Available at `https://arxiv.org/abs/1802.02942` (2018), 22 pages.
[40] *F. Gardini, G. Vacca*: Virtual element method for second-order elliptic eigenvalue problems. To appear in IMA J. Numer. Anal. doi
[41] *P. Grisvard*: Singularities in boundary value problems and exact controllability of hyperbolic systems. Optimization, Optimal Control and Partial Differential Equations (V. Barbu et al., eds.). Internat. Ser. Numer. Math. 107, Birkhäuser, Basel, 1992, pp. 77–84. zbl MR doi
[42] *E. K. U. Gross, R. M. Dreizler*: Density Functional Theory. Springer Science & Business Media 337, 2013. doi
[43] *T. Kato*: Perturbation Theory for Linear Operators. Grundlehren der Mathematischen Wissenschaften 132, Springer, Berlin, 1976. zbl MR
[44] *K. Lipnikov, G. Manzini, M. Shashkov*:, J. Comput. Phys. 257 (2014), 1163–1227 Mimetic finite difference method. zbl MR doi
[45] *L. Mascotto, I. Perugia, A. Pichler*: Non-conforming harmonic virtual element method: h-and p-versions. Available at `https://arxiv.org/abs/1801.00578` (2018), 27 pages.
[46] *D. Mora, G. Rivera, R. Rodríguez*: A virtual element method for the Steklov eigenvalue problem. Math. Models Methods Appl. Sci. *25* (2015), 1421–1445. zbl MR doi

[47] *D. Mora, G. Rivera, R. Rodríguez*: A posteriori error estimates for a virtual element method for the Steklov eigenvalue problem. Comput. Math. Appl. *74* (2017), 2172–2190. MR doi
[48] *D. Mora, G. Rivera, I. Velásquez*: A virtual element method for the vibration problem of Kirchhoff plates. To appear in ESAIM Math. Model. Numer. Anal. doi
[49] *D. Mora, I. Velásquez*: A virtual element method for the transmission eigenvalue problem. Available at `https://arxiv.org/abs/1803.01979` (2018), 24 pages.
[50] *J. E. Pask, B. M. Klein, P. A. Sterne, C. Y. Fong*: Finite-element methods in electronic-structure theory. Comput. Phys. Commun. *135* (2001), 1–34. zbl doi
[51] *J. E. Pask, P. A. Sterne*: Finite element methods in ab initio electronic structure calculations. Modelling Simul. Mater. Sci. Eng. *13* (2005), R71–R96. doi
[52] *J. E. Pask, N. Sukumar*: Partition of unity finite element method for quantum mechanical materials calculations. Extreme Mechanics Letters *11* (2017), 8–17. doi
[53] *J. E. Pask, N. Sukumar, M. Guney, W. Hu*: Partition-of-unity finite-element method for large scale quantum molecular dynamics on massively parallel computational platforms. Technical report LLNL-TR-470692, Department of Energy LDRD (2011); Available at `https://e-reports-ext.llnl.gov/pdf/471660.pdf`.
[54] *W. E. Pickett*: Pseudopotential methods in condensed matter applications. Computer Physics Reports *9* (1989), 115–197. doi
[55] *N. Sukumar, J. E. Pask*: Classical and enriched finite element formulations for Bloch-periodic boundary conditions. Int. J. Numer. Methods Eng. *77* (2009), 1121–1138. zbl MR doi
[56] *G. Vacca*: Virtual element methods for hyperbolic problems on polygonal meshes. Comput. Math. Appl. *74* (2017), 882–898. MR doi
[57] *G. Vacca*: An H^1-conforming virtual element for Darcy and Brinkman equations. Math. Models Methods Appl. Sci. *28* (2018), 159–194. zbl MR doi
[58] *P. Wriggers, W. T. Rust, B. D. Reddy*: A virtual element method for contact. Comput. Mech. *58* (2016), 1039–1050. zbl MR doi
[59] *W. Yang, P. W. Ayers*: Density-functional theory. Computational Medicinal Chemistry for Drug Discovery. CRC Press, Boca Raton, 2003, pp. 103–132.

Authors' addresses: *Ondřej Čertík*, Group CCS-2, Computer, Computational and Statistical Division, Los Alamos National Laboratory, Los Alamos, New Mexico – 87545, USA, e-mail: `certik@lanl.gov`; *Francesca Gardini*, Dipartimento di Matematica, Università degli Studi di Pavia, Via Ferrata, 5 – 27100 Pavia, Italy, e-mail: `francesca.gardini@unipv.it`; *Gianmarco Manzini*, Group T-5, Theoretical Division, Los Alamos National Laboratory, Los Alamos, New Mexico – 87545, USA, e-mail: `gmanzini@lanl.gov`; *Giuseppe Vacca*, Dipartimento di Matematica e Applicazioni, Università di Milano Bicocca, Via R. Cozzi, 55 – 20125 Milano, Italy, e-mail: `giuseppe.vacca@unimib.it`.